IN-HOST DENSITY-DEPENDENT MODEL OF HIGH-RISK HPV VIRIONS, BASAL CELLS AND LYMPHOCYTES T-CELLS INCORPORATING FUNCTIONAL RESPONSES

ELOSY MAKENA

A PROJECT SUBMITTED IN PARTIAL FULFILLMENT OF THE REQUIREMENTS FOR THE AWARD OF THE DEGREE OF MASTER OF SCIENCE IN APPLIED MATHEMATICS OF THE UNIVERSITY OF EMBU

SEPTEMBER, 2024

DECLARATION

This project is my original work and has not been presented for a degree or any other award.

Signature……. Date……

Elosy Makena
Department of Mathematics and Statistics
B527/1511/2021

This project has been submitted for examination with our approval as the University Supervisors.

Signature…… Date……

Dr. Patrick Kimani, PhD
Department of Mathematics and Statistics
University of Embu

Signature…… Date……..

Dr. Cyrus Gitonga Ngari, PhD
Department of Pure and Applied Sciences
Kirinyaga University

DEDICATION

Special dedication to my family, whose unwavering support and encouragement have been instrumental in my academic journey. To my friends and mentors, for their invaluable guidance and inspiration. Lastly, to all those who have supported and inspired me along the way, this achievement is as much yours as it is mine.

ACKNOWLEDGEMENT

Above all, I want to express my gratitude to God for giving me the courage, discernment, and persistence I needed to finish this study endeavor. It would not have been possible to accomplish this without His grace and direction.

I would also like to express my heartfelt gratitude to the University of Embu for awarding me the scholarship that made this research possible. Your generous support has been crucial in allowing me to pursue my academic goals. Special thanks to my supervisors, Dr. Cyrus Gitonga Ngari and Dr. Patrick Kimani for your invaluable guidance, support, and encouragement throughout this journey. Your insights and expertise have been instrumental in shaping this work. I extend my sincere gratitude to the reviewers and editors of the Heliyon journal, published by Elsevier, for their invaluable feedback and meticulous action to detail. Your constructive comments and suggestions have significantly enhanced the quality of this research. Your dedication to maintaining high standards of academic excellence is deeply appreciated. I am deeply grateful to my family and friends especially Jeremiah Kilonzi for educating me on how to use Matlab and for helping out in numerical simulation. Your confidence in me has served as a continuous source of inspiration. Lastly, I would like to acknowledge my colleagues and peers for their collaboration and constructive feedback, which have greatly contributed to the success of this project.

TABLE OF CONTENTS

LIST OF TABLES

LIST OF FIGURES

LIST OF APPENDICES

LIST OF ABBREVIATIONS AND ACRONYMS

HPV	Human Papilloma Virus
ODE	Ordinary Differential Equations
SDG	Sustainable Development Goals
STI	Sexually Transmitted Infection
UNDP	United Nations Development Program
VLP	Viral like particles
WHO	World Health Organization

DEFINITION OF TERMINOLOGIES

Antigen An antigen is a molecule that binds to an antibody or receptors on immune cells.

Apoptosis The death of cells that occur as normal and controlled.

Morbidity Having a disease or a symptom of the disease.

Parameter A variable that, within its range of possible values, indicates a group of unique occurrences within an issue.

Proliferation The process by which a cell grows and divides to produce two daughter cells.

Risk factors These are any attributes, characteristics, or exposure of an individual that increase the likelihood of developing a disease or injury. Anything that increases the chances of getting a disease such as cancer.

Viron A virus having a capsid and an RNA core that is entirely ineffectual when it is outside of a host cell. A virus can spread from one infected host cell to another host cell through its vector stage, or viron.

LIST OF SYMBOLS

Θ	Theta
η	neta
β	beta
λ	lambda
ρ	rho
ω	omega
α	alpha
δ	delta
ϵ	epsilon

ABSTRACT

Cervical cancer is one of the most common types of cancer and it is caused mostly by high-risk Human Papillomavirus (HPV) and continues to spread at an alarming rate. While HPV impacts have been investigated before, there are currently only a scanty number of mathematical models that account for HPV's dynamic role in cervical cancer. The objectives were to develop an in-host density-dependent deterministic model for the dynamics implications of basal cells, virions, and lymphocytes incorporating immunity and functional responses. Analyze the model using techniques of epidemiological models such as basic reproduction number and simulate the model using Matlab ODE solver. Six compartments are considered in the model that is; Susceptible cells (S), Infected cells (I), Precancerous cells (P), Cancerous cells (C), Virions (V), and Lymphocytes (L). Next generation matrix (NGM), survival function, and characteristic polynomial method were used to determine the basic reproduction number denoted as R_0. The findings from this research indicated that the Disease-Free Equilibrium point is locally asymptotically stable whenever $R_0^* < 1$ and globally asymptotically stable if $R_0^* \leq 1$ and the Endemic Equilibrium is globally asymptotically stable if $R_0^* > 1$. The results obtained show that the progression rate of precancerous cells to cancerous cells (θ) has the most direct impact on the model. The model was able to estimate the longevity of a patient as 10 days when (θ) increases by 8%. The findings of this research will help healthcare providers, public authorities, and non-governmental health groups in creating effective prevention strategies to slow the development of cervical cancer. More research should be done to determine the exact number of cancerous cells that can lead to the death of a cervical cancer patient since this paper estimated a proportion of 75%.

Keywords: In-host model, functional responses, stability analysis, simulation and reproduction number.

CHAPTER ONE

INTRODUCTION

1.1 Background information.

Cancer is a medical condition in which the cells in the body proliferate abnormally. Cervical cancer is the uncontrolled invasive growth of the epithelial cells in the cervix, which is the lower part of the uterus that connects to the vagina (Chakraborty, Cao, et al., 2019). The main cause of most cervical cancer is Human Papillomavirus and HPV infection is involved in the development of cervical cancer in more than 90 percent of cases (Chakraborty, Cao, et al., 2019).

Human papillomavirus (HPV) is the most common sexually transmitted infection worldwide, with a particularly high prevalence in sexually active individuals. HPV is is passed through skin-to-skin contact. This is often through a cut, abrasion, or a small tear in the skin and sexual activity without protection.

Human papillomaviruses (HPV) are small double-stranded DNA viruses that have a diameter of 52-55 nm. There are over 200 types of HPV, categorized into "low-risk" and "high-risk" types. Low-risk HPV types, such as HPV 6 and 11, are primarily associated with benign conditions like genital warts. In contrast, high-risk HPV types, especially HPV 16 and 18 are responsible for the majority of HPV-related cancers, including cervical cancer, anal cancer, and oropharyngeal cancers.

Cervical cancer is among the leading causes of morbidity and mortality globally. World Health Organization (WHO) fact sheet of 2018 reported that in 2018, around 311,000 women globally lost their lives to cervical cancer, with an estimated 570,000 women receiving a diagnosis. Therefore, cervical cancer is a global health concern and ranks as the fourth most frequent female malignancy worldwide (Kessler, 2017). World Health Organization fact sheet of 2010 reported that cervical cancer is the second most frequent cancer after breast cancer in Kenya among women between the ages of 15 to 44 years. Cervical cancer remains a significant health issue in Kenya, contributing heavily to the cancer burden. It is the second most prevalent cancer among women, and about nine women die from cervical cancer every day. This high mortality rate is primarily due to late-stage diagnosis and limited access to timely

screening and treatment services. In 2020, Kenya recorded 42,000 new cancer cases, with cervical cancer accounting for a considerable portion of these cases. As of 2023, cervical and breast cancers together make up 23% of all cancer-related deaths in the country.

Every woman is prone to cervical cancer, but most often it occurs in people over 30 years of age. As long as there is prompt identification, the immune system typically clears the majority of HPV cases in women within a year (Ryser *et al.*, 2015). This is normally aided by lymphocyte cells. Lymphocytes are a type of white blood cells that help the body's immune system to fight cancer, foreign virus, and bacteria. T-lymphocytes are responsible for annihilating virus-infected cells (Kathleen & Summers, 2020). The immune system combines the body's identification of foreign substances and its defense mechanism against them. Key players in the immune system are several types of white blood cells, such as lymphocytes.

T-lymphocytes are responsible for annihilating virus-infected cells (Kathleen & Summers, 2020). Yet during sexual activity, viruses like HPV take advantage of abrasion of the vaginal or oral mucosa's epidermal lining (Verma *et al*., 2017) to enter the body. Due to their immune-evasive behavior, diseases like HPV make it very difficult for the immune response to be activated (Mondaini *et al.*, 2021).

Some of the risk factors of cervical cancer include tobacco usage, harmful alcohol consumption, overweight, obesity, age, the individual's sex, and genetic or inherited factors. Exposure to carcinogens in the environment, such as chemicals, radiation, and infectious agents, is a concern (F.Getum, *et al.*, 2013).

The dynamics of HPV to cervical cancer are clearly shown in Figure 1 (Stark & Zivković, 2018).

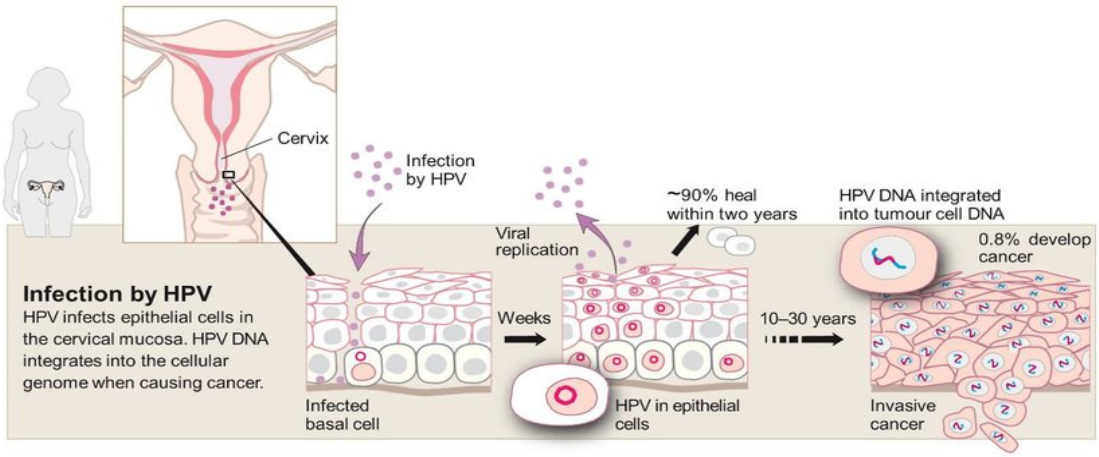

Figure 1: Progression of cervical cancer by HPV

A mathematical model is a created micro world where entities act by well-defined rules and presumptions. We can investigate the general behavior of a mathematical model and determine the implications of our assumptions by doing mathematical analysis, which is frequently supported by computer simulations (Huppert & Katriel, 2013). In-host mathematical models are used to describe how interactions between virus particles, host cells, and the immune system affect the viral load over time.

No population can grow exponentially all the time. Many populations initially grow exponentially but due to competition for food and territory among other resources, the population size levels off after some time to a stable size K which is the carrying capacity. The carrying capacity (K) represents the highest population that the ecosystem is capable of supporting steadily (Weiss, 2009).

The exponential model has drawbacks when used to forecast the long-term growth rate of cancer cell proliferation, therefore a logistic model was developed to address these issues and describe the behavior of cancer cell growth and proliferation. According to the logistic model equation, growth increases proportionally and linearly with cell size until it reaches its carrying capacity. For the volume of a cancer cell, a logistic equation yields an S-shaped curve (Tabassum *et al*., 2019).

1.2 Statement of problem.

Cervical cancer is among the leading diseases causing mortality worldwide with an estimate of 342,000 deaths in 2020. Sustainable Development Goals (SDG) targets 3.4 and 5 to reduce premature mortality from non-communicable diseases (NCDs) by a third by 2030 relative to 2015 levels, to promote mental health and well-being, and

to achieve gender equality and empower all women and girls respectively (Online & Ezzati, 2020), there is need to focus on women's health.

Most previous studies have modeled cervical cancer progression at the population level, using frameworks such as the $SI_{HPV}, I_{UC}, and\ I_{CC}$ models (Pongsumpun, 2012a), among others. While these models provide valuable insights into the spread of HPV and its connection to cervical cancer, they overlook critical aspects when focusing on the host cell level. Studies that modeled HPV dynamics in terms of host cells, such as the SIVPC model (Chakraborty, Cao, et al., 2019), did not account for important factors like density-dependent cell populations, functional responses, or the maximum number of cancerous cells that lead to host mortality.

To address these gaps, a new mathematical model was developed. This model focuses on in-host dynamics, incorporating density-dependent interactions between basal cells, virions, and lymphocytes, and examines their relation to cervical cancer progression. The model was analyzed using epidemiological techniques and simulated using Matlab's built-in ODE solver.

1.3 Research Questions

1. What is the logistic deterministic model of basal cells, virions, and lymphocytes incorporating the immune and functional response?

2. What is the ill-posedness or the well-posedness of the proposed model?

3. What are the simulated results of the model using Matlab inbuilt ordinary differential equations (ODE) solver?

1.4 Objectives of the Study

1.4.1 General Objectives

To develop an in-host logistic mathematical model for basal cells, virions, and lymphocytes and simulate their dynamics to cervical cancer using Matlab inbuilt ODE solver.

1.4.2 Specific Objectives

The specific objectives are to:

1. Develop an in-host logistic deterministic model for basal cells, virions, and lymphocyte dynamics implications on cervical cancer in the presence of immune and functional response.
2. Analyze the model using techniques of epidemiological models such as basic reproduction number, positivity, and determining equilibrium points and their stabilities.
3. Simulate the model using Matlab inbuilt ODE solver which is based on the Runge-Kutta method.

1.5 Justification of the Study

Cervical cancer disease is a major challenge globally today. Roughly 90% of deaths from cervical cancer take place in less developed parts of the globe. The socioeconomic effects of cervical cancer are severe since African women are primarily affected at a relatively young age (LaVigne & Leitao, 2019).

The study on Human Papillomavirus dynamics to cervical cancer using first-order nonlinear ordinary differential equations is of great significance since the findings of this study will provide information to individuals and also to the health community concerning the spread of cervical cancer and recommend necessary measures that will help mitigate the future spread of HPV and cervical cancer.

1.6 Scope of the Study

Other risk factors contribute to causes of cervical cancer, but the primary risk factor is Human Papillomavirus (HPV) infection (Ault, 2006). Since HPV infection is essentially an STI, several risk factors for cervical cancer are also linked to a higher chance of STI occurrence (LaVigne & Leitao, 2019). To model the dynamics of cervical cancer, this study is restricted to the Human Papillomavirus infection as the primary cause considering the in-host logistic deterministic model of basal cells, virions, and lymphocytes.

CHAPTER TWO

REVIEW OF LITERATURE

2.1 Introduction

To provide some insights into this study, this section brings to light relevant literature. In particular, literature that is based on mathematical modeling of Human Papillomavirus dynamics. It focuses on methods to stop the spread of latent infections, immunization, early diagnosis, education counseling, treatment of drug-resistant strains, and the effects of awareness. Finally, the focus is directed on current research that will attempt to fill the gap in the literature.

2.2 Dynamics of HPV on cervical cancer

Pongsumpun (2012) used a deterministic mathematical model system of ODE and numerical simulation to investigate the dynamics of cervical cancer. The total population was subdivided into five compartments namely; susceptible (S), vaccinated (V), infected(I), permanently recovered (R_P), and temporarily recovered(R_T). It was evident that cervical cancer infection can be eradicated by increasing the recovery rate and eliminated by decreasing the contact rate in the presence of vaccination. It was concluded that the number of infected people keeps decreasing if vaccination is combined with appropriate treatment.

Asih *et al.* (2016) applied a $SIVPC$ mathematical model consisting of 5 compartments which include: Susceptible (normal) cells (S), Infected cells(I), Free virus(V), Precancerous cells(P), and Cancer cells(C). The study's goal was to examine the transition of cervical cells from normal to precancerous and cancerous states. According to the analysis, the solution settles into a steady state with a small number of precancerous cells (long-term control) and the precancerous cell population expanding without limit and serving as a rich source of new cancer cells (malignancy). Based on the findings, it was determined that drug-based preventative measures for cervical cancer may be implemented. It was suggested that more relevant biology, such as the immune system, may be included in models to help them become more accurate.

Chakraborty *et al*. (2019) applied a $SIVPC$-based mathematical model with five compartments -susceptible cells(S), infected cells (I), HPV virus(V), precancerous

cells(P), and cancerous cells(C). The goal of the research was to characterize how the four types of epithelial and basal cells interact with the human papillomavirus. The findings suggest that the malignant cell population expands linearly for Holling type 1 functional response, which is an unlikely scenario. After concluding that a Holling type III functional response is more likely to occur in precancerous cervical cells, it was recommended that the model be utilized by combining the three control measures, employing one immunization and one treatment to reduce the spread of cervical cancer (tumor suppressive drug).

Asih *et al.* (2019) formulated a cusp bifurcation on the cervical cancer mathematical model using two parameters from previous studies. The study's goal was to find a cusp bifurcation by combining a continuation of the maximal invasion rate parameter with a continuation of the infection rate. It has been observed that the parameters (the infection rate) and (the maximal invasion rate) are evolving into bifurcation parameters. It was concluded that the rate of infection was a major component in the development of cervical cancer and that the invasion rate was also crucial. It was recommended that future studies might focus on determining infection rates and maximal invasion levels in advance.

Kaur *et al.* (2022) created a mathematical model using the ordinary least squares (OLS) regression method to study cervical cancer and the different risk factors that lead to the development of the disease. The objective of the study was to create a set of mathematical relationships between the two risk categories for cervical cancer: low risk and high risk.

When the model was examined, it was found that the main factors that predict cervical cancer are Schiller, Heinselman, and Cytology. It was also found that visceral fat is a health indicator that is a fantastic predictor of an individual's health when doing casual root analysis with alternative variables, but only the self-influencing ones were included in the analysis.

Sierra-Rojas *et al.* (2022) proposed a deterministic model of the epithelial cellular dynamics of the stratified epithelium of three stratums- Stratum Basale($BH\ (t)$), Stratum intermedium ($EH\ (t)$) and Stratum corneum ($CH\ (t)$) based on three ordinary differential equations. The purpose of this investigation was to simulate HPV's behavior in cervical epithelial cells. Based on the results of the model, it is

clear that antiviral medications aimed at preventing new viral infections and inhibiting viral replication are necessary to bring down the viral transmission rate and the viral production rate. It was concluded that the model does not take into account the four layers that make up the stratified epithelium.

2.3 Immunization and Treatment

Kivuti-bitok *et al.* (2015) created a mathematical model of cervical cancer in women and investigated the impact of different preventative measures. The model predicted that the prevalence of HPV/cervical cancer is not zero, indicating that it is an epidemiological illness with a long time horizon. The researchers applied dynamical modeling in which differential equations along with boundary conditions were formulated.

The researchers concluded that the model accurately anticipated realistic expectations for the development of both diagnosed and undiagnosed cervical cancer, mortality from cervical cancer, and plausible epidemiological trends accounting for the effects of the different treatments. Due to its dynamic nature, the model may be modified as more data becomes available.

Ndii (2020) formulated a $SIVPCM$ mathematical model with six compartments-susceptible cell density(S), infected cell density(I), virus density(V), precancerous cell density(P), cancer cell density(C), and concentration of chemotherapy drugs(M)). The purpose of this research was to report on the efficacy of chemotherapy in treating cervical cancer. Although it has the unfortunate side effect of killing normal cells like those lining the mouth and intestines or those that control growth, this study indicated that chemotherapy is efficient enough to destroy aberrant cells like those caused by infection, precancerous, and cancer. Therefore, it was found that while chemotherapy is fairly helpful in treating cervical cancer, additional research into more effective therapies is required particularly to lessen the negative effects on normal cells.

Zhang *et al.* (2020) constructed a mathematical model of HPV natural history that was divided into six compartments: susceptible individuals (S), asymptomatic infectious individuals (E), symptomatic infectious individuals (I_1), individuals with persistent HPV infection (I_2), cancer-infected individuals (A), and recovered

individuals (R). The model was used to qualitatively analyze the stability of disease-free equilibrium, the non-existence of a limit cycle, and the existence of forward bifurcation.

The results showed that the contact rate of $E\ (t)$ with $S\ (t)$ increased as the number of infected individuals increased, consequently, the increased contact rate increased the disease outbreak. It was concluded that when R_0<1 the disease would die out and when $R_0 > 1$ the infection would experience an outbreak.

Chakraborty *et al*. (2020) developed a mathematical model of cervical cancer dynamics at the cellular level to describe the interaction between cancerous cells, natural killer (NK), effector T cells, and Human Papillomaviruses (HPV). The study aimed to understand how lymphocytes specifically the NK cells and effector T cells defend the body's immunity against cancer cells and HPVs. From the results obtained, it was evident that NK and effector T cells are responsible for eradicating cervical cancer which is induced by HPV, but it was important to enhance their destruction power. It was concluded that NK and effector T cell-based immunotherapy holds great promise for cancer treatment.

Akgül *et al.* (2021) constructed a compartmental model to investigate women's malignant disease, cervical cancer. The aim was to discuss the transmission and persistence of cervical cancer in the community using the fractal fractional model. From the results the number of populaces $I_{HPV}\ (t)$ and $I_{CC}\ (t)$ approaches zero as time grows, on the other hand, the whole population becomes susceptible at that stage. It was proposed that the scheme can be applied efficiently on extended fractal fractional predator-prey models, chemical reaction models, and reaction-diffusion models.

Previous studies have overlooked key aspects of cervical cancer progression at the cellular level, such as density-dependent cell populations, functional responses, and the maximum threshold of cancerous cells that result in host mortality. To address these gaps, a new mathematical model was developed that captures the in-host dynamics of cervical cancer. This model incorporates density-dependent interactions between basal cells, virions, and lymphocytes, simulating their roles in cancer progression. The model was analyzed using epidemiological techniques and

simulated with Matlab's built-in ODE solver to provide deeper insights into disease dynamics.

CHAPTER THREE

RESEARCH METHODOLOGY

3.1 Introduction

The goal of the project was to create an in-host density-dependent deterministic model that explains how the dynamics of cervical cancer are affected by the Human Papillomavirus, basal cells, and lymphocytes. The population of basal layer cells was divided into five compartments for the study. Five first-order nonlinear ordinary differential equations will be used to represent the progression from one compartment to another. The logistic equation is expressed as; $\frac{dV}{dt} = aV\left(1 - \frac{V}{b}\right)$, where, b is the carrying capacity (Tabassum *et al*., 2019).

The Michaelis-Merten reaction or the Monod response are other names for this functional response. For predators with a Holling Type II functional response, the rate of prey consumption increases with the size of the prey population but saturates at some maximum level A.

The general equation for Holling Type II functional response is $\frac{AN}{B+N}$ (Weiss, 2009).

For Holling Type III, the functional response $\frac{AN^2}{B^2+N^2}$, where B is the switching value. This response is characteristic of predators that are below a certain prey density threshold, and do not eat much of the prey, but when the prey density is above the threshold, their feeding rate increases as the prey population increases, but eventually levels off to an asymptote (Weiss, 2009).

Arditi-Ginzburg functional response $\frac{AN}{N+BP}$ believes that the amount of prey consumed by each predator in a given amount of time is only determined by the amount of prey present. Nevertheless, it is recognized that predator density can also affect the pace at which each individual consumes food, an effect known as predator reliance (Weiss, 2009).

3.2 Methods

In this study, first-order nonlinear ordinary differential equations were used to create a logistic deterministic model for the effects of the Human Papillomavirus. The model of HPV infection and cancer development considered 6 compartments namely: S-

Susceptible (normal) cells, I-Infected cells, V-Free virus, P-Precancerous cells, C-Cancerous cells and L- Lymphocytes cells. The model will be analyzed in terms of positivity, equilibrium points, and their stabilities and the basic reproduction number will be determined using the next-generation matrix method.

3.3 Proposed Model Description.

3.3.1 Basal cell population.

The population of basal cells was divided into four compartments namely: Susceptible cells (S), Infected cells (I), Precancerous cells (P), and cancerous cells (C). The total population of basal cells N (t) is given by, $N(t) = S(t) + I(t) + P(t) + C(t)$. All basal cells undergo a natural death rate at δ_1, a logistic growth at a rate of r_1, and a carrying capacity of K.

HPV invades the human body through small micro-abrasions that sometimes occur in the cervical epithelium and infect the basal layer cells at the rate of λ_1. All cells increase from logistic cell growth. The number of infected cells decreases at the rate η_1 which is the induced death rate. HPV infection can be autoimmune and some infected cells again become susceptible. The infected cells become precancerous at a progression rate β. When the infected cells become precancerous, there is a risk of developing cancer. When the population of precancerous cells is at a low level, there is a small risk of developing cancer cells. The transition from precancerous to cancerous cells was considered to be governed by a saturating term $f(P) = \frac{CP^2}{D^2+P^2}$ according to whether the risk is high or low and the progression risk as θ.

3.3.2 Virion Population.

Virions grow logistically at a rate of r_2 and undergo normal death at a rate δ_2. New HPV virions are produced at a rate η_1, η_2, and η_3 proportional to the induced death rate of the infected, precancerous, and cancerous cells respectively.

3.3.3 Lymphocyte Population.

Lymphocytes also grow logistically at a rate of r_3 and undergo a natural death (apoptosis) at a rate δ_3.

3.4 Assumptions of the Model

Besides the common assumptions of any epidemiological model, the following are additional assumptions.This study assumed that: the number of cervical epithelial cells remains roughly constant, and the epithelium is replaced every 4-5 days (Engida Sado, 2019); All the epithelium cells are susceptible; The basal cell population grows logistically, with an intrinsic growth rate and a carrying capacity; There is significance to the recovery from natural immunity and Human Papilloma Virus infection is the strongest risk factor for cervical cancer.

(i) $\frac{AS}{S+BV}$ is Arditi-Ginzburg function predator (virions) density can also influence individual (Prey/Basal Cells) consumption rate, an effect termed predator dependence. The ratio of prey density to predator density will determine how virions attack Basal cells.

(ii) $\frac{CP^2}{D^2+P^2}$ is a saturation function based on Holling type III response.

(iii) $\frac{EM}{F+M}$ is based on Holling type II response on the assumption that the rate of infected basal cell recovery increases with the immunity level, but saturates at some maximum level A.

3.5 Description of Variables and Parameters

Table 1: Variables Description

Variables	**Description**
S(t)	Susceptible cells at time t.
I(t)	Infected cells at time t.
P(t)	Precancerous cells at time t.
C(t)	Cancerous cells at time t.
V(t)	Virions population at time t.
L(t)	Lymphocytes population at time t.

Table 1: Description of variables

Table 2: Parameters Description

Parameters	Description
r_1	Mitosis division rate of basal cells
r_2	Division rate of virons
r_3	Division rate of lymphocytes
K_1	Carrying capacity of basal cells
K_2	Carrying capacity of virons
K_3	Carrying capacity of lymphocytes
K_4	The population of cancerous cells that causes a person to die
τ_2	The rate of infection of susceptible cells by virus
β	Progression rate from infected cells to precancerous cells
θ	Progression rate from precancerous cells to cancerous cells
η_1	The induced death rate of infected cells
η_2	The induced death rate of precancerous cells
η_3	The induced death rate of cancerous cells
δ_1 , δ_2, δ_3	The apoptosis rate of basal cells, virons and lymphocytes respectively
D	Half-saturation concentration for the progression from P to C
$\omega_1, \omega_2, \omega_3$	Number of virons that are produced by I, P and C respectively
M	The autoimmune rate of I to S
α_1	Contact rate
ϵ	Rate at which the virons are killed by the lymphocytes
τ_1	Rate at which virons are eliminated as they attack normal cells

Table 2: Description of parameters

3.6 Proposed model flow chart and equations

3.6.1 The proposed model flow chart

.

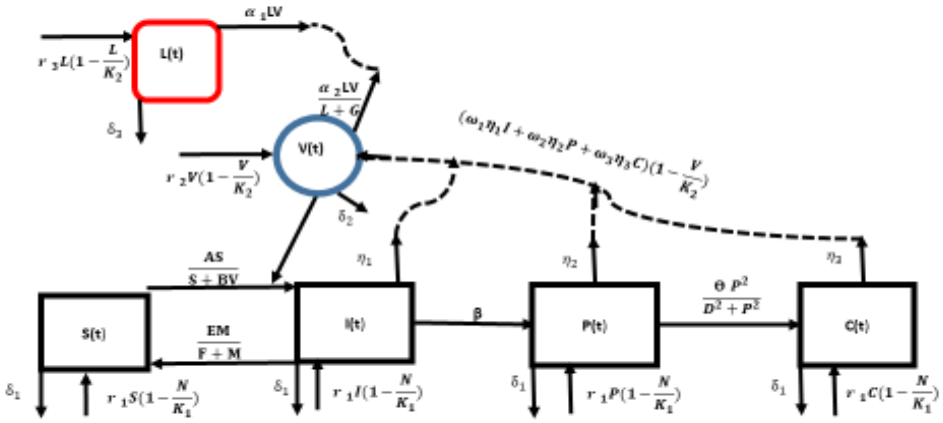

Figure 2: Model flow chart

3.6.2 Model equations

$$\frac{ds}{dt} = r_1 S\left(1 - \frac{N}{K_1}\right) - \frac{AS}{S+BV} + \frac{EM}{F+M} I - \delta_1 S,$$

$$\frac{dI}{dt} = r_1 I\left(1 - \frac{N}{K_1}\right) + \frac{AS}{S+BV} - \beta I - \frac{EM}{F+M} I - \eta_1 I - \delta_1 I,$$

$$\frac{dP}{dt} = r_1 P\left(1 - \frac{N}{K_1}\right) + \beta I - \theta \frac{CP^2}{D^2+P^2} - \eta_2 P - \delta_1 P,$$

$$\frac{dC}{dt} = \left\{r_1 C\left(1 - \frac{N}{K_1}\right) + \theta \frac{CP^2}{D^2+P^2} - \eta_3 C - \delta_1 C\right\}\left(1 - \frac{C}{K_4}\right),$$

$$\frac{dV}{dt} = \{r_2 V + \omega_1\eta_1 I + \omega_2\eta_2 P + \omega_3\eta_3 C\}\left(1 - \frac{V}{K_2}\right) - \epsilon \frac{L}{L+K_4} V - \delta_2 V,$$

$$\frac{dL}{dst} = r_3 L\left(1 - \frac{L}{K_3}\right) - \alpha_1 LV - \delta_3 L.$$

Where $A = \tau_2$

3.7 Model Analysis

The model was examined by demonstrating several theorems, including those about the model's positivity and invariant region, equilibrium points, reproduction number, and stabilities.

3.7.1 Positivity and invariant region

If the region $R = \{S(t), I(t), P(t), C(t), V(t) and\ L(t)\} \in R6$ and $S(0) \geq 0, I(0) \geq 0, P(0) \geq 0, C(0) \geq 0, V(0) \geq 0, L(0) \geq 0$ then the region is positively bounded. Concerning systems of equations (1)-(6), was attracted to and positively invariant.

3.7.2 Equilibrium point

When the differentials are equal to zero, a system is considered to be in equilibrium. A positive endemic equilibrium existed if and only if $R_C > 1$, and the disease-free equilibrium of the system (1) through (5) was reached by equating all susceptible, infectious, precancerous, and cancerous to zero (Krakauer, 2009).

3.7.3 Basic reproduction number R_0 and control reproduction number R_C

When an individual with the virus is brought into contact with a population that is completely vulnerable, the fundamental reproduction number, R_0, is the total number of secondary infections that result throughout an episode of the illness. To calculate the model's basic reproduction number (R_0) and control reproduction number (R_C), this study employed the next-generation matrix approach (Afolabi *et al*., 2021). The transfer of infectious terms from one compartment to another was represented, respectively, by the non-negative matrix F and non-singular matrix V (At DFE). Thus,

$F = [\partial F_i\,(X_i\,)/\partial\, X_i]$ and $V = [\partial V_i\,(X_i)/\partial X_{\,i}]$.

The largest Eigenvalue of the matrix (FV^{-1}) is the value of the reproductive number.

3.7.4 Stabilities of the Equilibrium Point

Stability is the state in which an equilibrium point remains constant across time. Stability can take two distinct forms: global stability and local stability. A local stable equilibrium point is one where all the neighbors of the equilibrium point steadily move in that direction over time. Furthermore, the equilibrium point is seen as globally stable if all of the system's components progressively move in that way over time.

We first determined the local stability of DFE using the Jacobian of the model tested at DFE. Next, we determined the stability of this steady state using the related Jacobian, which is a function of the model parameters. Finally, we evaluated the global stability of DFE using the Lyapunov function (Bershadsky *et al*., 2019).

3.7.5 Bifurcation analysis

The possibility of bifurcation in the model was indicated by the possible presence of two endemic equilibriums. The study used the center manifold theory to carry out the bifurcation analysis (Kumar & Nilam, 2019).

3.8 Numerical simulation

To further understand the effect of effective contact rate on transmission dynamics of implications of human papillomavirus infections, a numerical simulation of the model was run using the inbuilt ODE solvers in MATLAB software.

3.9 Normalized sensitivity analysis

Sensitivity analysis helps us assess the relative change in state variables when a parameter changes. This will enable us to forecast a system's dynamics. This was done based on the basic reproduction number.

The sensitivity is given by: $Sensitivity = \frac{\%\ change\ of\ output}{\%\ change\ of\ input}$ (Norton, 2008).

CHAPTER FOUR

RESULTS AND INTERPRETATION

This chapter presents the study's findings and interpretation. It has been suggested to numerically simulate the model using assumptions and data from the literature review. In this chapter, sensitivity indices are also displayed.

This section is organized as follows: 4.1. Model analysis and 4.2 Model simulation.

4.1 Model Analysis

This sub-section is organized as follows: **4.1.1** Existence and positive in variance, **4.1.2.** Boundedness of the solution, **4.1.3** Disease-free equilibrium point, **4.1.4** Basic reproduction number, **4.1.5** Endemic equilibrium, **4.1.6** Stability analysis, and **4.1.7** Bifurcation analysis.

4.1.1 Existence and positive invariance

Theorem 1: Solutions of the model equations (1) – (6) together with the initial conditions $S(0) \geq 0, I(0) \geq 0, P(0) \geq 0, C(0) \geq 0, V(0) \geq 0, L(0) \geq 0$ are always positive or the model variables $S\,(t)$, $I(\,t)$, P(t), C(t), V(t) and L(t) all positive for all t and will remain in R_6^+ (Gurmu & Koya, 2019).

Proof

For the sake of analysis

$$\frac{dS}{dt} = r_1 S(1 - k_1 N) - \frac{\tau_2 SV}{S+BV} + \Omega_1 I - \delta_1 S, \tag{7}$$

$$\frac{dI}{dt} = r_1 I(1 - k_1 N) + \frac{\tau_2 S}{S+BV} - \Omega_2 I, \tag{8}$$

$$\frac{dP}{dt} = r_1 P(1 - k_1 N) + \beta I - \theta \frac{CP^2}{D^2+P^2} - \Omega_3 P, \tag{9}$$

$$\frac{dC}{dt} = \left\{r_1 C(1 - k_1 N) + \theta \frac{CP^2}{D^2+P^2} - \Omega_4 C\right\}(1 - k_4 C), \quad . \tag{10}$$

$$\frac{dV}{dt} = \{r_2 V + \omega_1\eta_1 I + \omega_2\eta_2 P + \omega_3\eta_3 C\}(1 - k_2 V) - \tau_1 SV - \epsilon \frac{L}{L+K_4} V - \delta_2 V, \tag{11}$$

$$\frac{dL}{dt} = r_3 L(1 - k_3 L) - \alpha_1 LV - \delta_3 L, \tag{12}$$

Where

$$\frac{1}{K_1} = k_1; \frac{1}{K_2} = k_2; \frac{1}{K_3} = k_3; \frac{EM}{F+M} = \Omega_1; \Omega_2 = \beta + \Omega_1 + \eta_1 + \delta_1; \Omega_3 = \eta_2 + \delta_1$$

$\Omega_4 = \eta_3 +$, to reduce the number of parameters, therefore;

For $t > 0$, let $W = (s(t), i(t), p(t), n(t), v(t), l(t))^T$ and $F(W) = (F1(W), F2(W), F3(W), F4(W), F5(W), F6(W))^T$,where $F1(W) = r_1 S(1 - k_1 N) - \frac{\tau_2 SV}{S+BV} + \Omega_1 I - \delta_1 S$, $F2(W) = r_1 I(1 - k_1 N) + \frac{\tau_2 SV}{S+BV} - \Omega_2 I, F3(W) = r_1 P(1 - k_1 N) + \beta I - \Theta \frac{CP^2}{D^2+P^2} - \Omega_3 P, F4(W) = \left\{r_1 C(1 - k_1 N) + \Theta \frac{CP^2}{D^2+P^2} - \Omega_4 C\right\}(1 - k_4 C), F5(W) = \{r_2 V + \omega_1 \eta_1 I + \omega_2 \eta_2 P + \omega_3 \eta_3 C\}(1 - k_2 V) - \tau_1 SV - \epsilon \frac{L}{L+K_4} V - \delta_2 V, F6(W) = r_3 L(1 - k_3 L) - \alpha_1 LV - \delta_3 L$. Then, the system (1)-(6) can be written as $\frac{dQ}{dt} = F(W)$ where $F: C_+ \to (R)_+^6$ with $W(0) = W_0 \epsilon R_+^6$. Thus, the function W is locally Lipschitzian and completely stable on R_+^6.

Therefore, the solution of the system with non-negative initial conditions exists and is unique. It is also evident that these solutions exist for all $t > 0$ and are non-negative, hence the region R_+^6 is an invariant domain of the system (Belew & Melese, 2022).

4.1.2 Boundedness of the solution

For the system to be mathematically meaningful, it is necessary to show that its state variables are positive and bounded for all t. That is, the solution of the system with a positive initial value will remain positive for all $t \geq 0$.

Theorem 2: The positive solutions of the system of model equations (1)-(6) are bounded. That is, the model variables S(t), I(t), P(t), C(t), V(t) and L(t) are bounded for all t (Gurmu & Koya, 2019).

Proof

$$N(t) = S(t) + I(t) + P(t) + C(t) \tag{13}$$

By differentiating equation (13) gives,

$$\frac{dN}{dt} = \frac{dS}{dt} + \frac{dI}{dt} + \frac{dP}{dt} + \frac{dC}{dt} \tag{14}$$

$$\frac{dN}{dt} = r_1 S\left(1 - \frac{N}{K_1}\right) - \delta_1 S + r_1 I\left(1 - \frac{N}{K_1}\right) - \eta_1 I - \delta_1 I + r_1 P\left(1 - \frac{N}{K_1}\right) - \eta_2 P -$$

$$\delta_1 P + r_1 C\left(1 - \frac{N}{K_1}\right) - \eta_3 C - \delta_1 C(1 - \frac{C}{K_4}) \quad (15)$$

$$\frac{dN}{dt} = r_1 N\left(1 - \frac{N}{K_1}\right) - (\ \delta_1 S + \eta_1 I + \delta_1 I + \eta_2 P + \delta_1 P + \eta_3 C + \delta_1 C(1 - \frac{C}{K_4})) \quad (16)$$

$$\frac{dN}{dt} \leq r_1 N\left(1 - \frac{N}{K_1}\right)$$

By using the separation of variables of inequality, we have $\frac{dN}{N\left(1-\frac{N}{K_1}\right)} \leq r_1 dt$ (17)

On integrating both sides (17) and applying the initial conditions to get the value of A and finally substituting the value of A, we have $N(t) \leq \frac{K_1}{1+(\frac{K_1}{N(0)}-1)e^{-rt}}$. (18)

Introducing limits, $\lim_{t\to\infty} N(t) \leq K_1$.Implying that $0 \leq N(t) \leq K_1$

Also for, $V(t)$

$$\frac{dV}{dt} = \{r_2 V + \omega_1\eta_1 I + \omega_2\eta_2 P + \omega_3\eta_3 C\}\left(1 - \frac{V}{K_2}\right) - \tau_1 SV - \epsilon\frac{L}{L+K_4}V - \delta_2 V. \quad (19)$$

Let $r_2 V + \omega_1\eta_1 I + \omega_2\eta_2 P + \omega_3\eta_3 C = r_4 V$ (20)

$\frac{dV}{dt} = r_4 V\left(1 - \frac{V}{K_2}\right) - \tau_1 SV - \epsilon\frac{L}{L+K_4}V - \delta_2 V$, then, $\frac{dV}{dt} \leq r_4 V\left(1 - \frac{V}{K_2}\right)$ (21)

By separating variables (21), integrating and applying initial conditions and limits we obtained $\lim_{t\to\infty} V(t) \leq K_2$.Therefore; $V(t) \leq K_2$ .Implying that, $0 \leq V(t) \leq K_2$.

Similarly, $L(t)$, $\frac{dL}{dt} \leq r_3 L\left(1 - \frac{L}{K_3}\right)$. Therefore; $L(t) \leq \frac{K_3}{1+(\frac{K_3}{L(0)}-1)e^{-rt}}$. On applying the limits as $t \to \infty$, it follows that; $0 \leq L(t) \leq K_3$.

4.1.3 Disease-free equilibrium point (DFE)

Theorem 3: The system of equation (1) to (6) has disease-free equilibrium point(E^0) obtained as; $E^0 = (S^0, I^0, P^0, C^0, V^0, L^0) = \left(\frac{K_1(r_1-\delta_1)}{r_1}, 0,0,0,0, \frac{K_3}{r_3}(r_3 - \delta_3)\right)$.

Proof

DFE of the system (1)-(6) is obtained by setting the right-hand side to zero and equating the infectious classes to zero $I = 0, P = 0, C = 0, A = 0\ and\ V = 0$ (Mutua et al., 2022).

Solving, we obtained. $S^0 = 0$ and $S^0 = \frac{K_1(r_1-\delta_1)}{r_1}$ $\mathrm{L}^0 = 0$ and $\mathrm{L}^0 = \frac{\mathrm{K_3(r_3-\delta_3)}}{\mathrm{r_3}}$. The set, $S^0 = \mathrm{L}^0 = 0$ was not biologically meaningful because it is not feasible to have a cervix with no basal cells and Lymphocytes. Hence $S^0 = \frac{K_1(r_1-\delta_1)}{r_1}$ and $\mathrm{L}^0 = \frac{\mathrm{K_3(r_3-\delta_3)}}{\mathrm{r_3}}$. Hence the disease-free equilibrium point of the system of equations (1) to (8) was obtained as:

$$E^0 = (S^0, I^0, P^0, C^0, V^0, L^0) = \left(\frac{K_1(r_1-\delta_1)}{r_1}, 0,0,0,0, \frac{K_3}{r_3}(r_3-\delta_3)\right).$$

4.1.4 Basic reproduction number (R_0)

There are numerous controversies surrounding the method of calculating basic reproduction number(R_0) because it has been proven that each method produces a unique estimate of (R_0) hence posing a challenge to stakeholders on how best to control the dynamics of a disease (Smith et al., 2011)**.** Although most studies have evaluated R_0 using the next-generation method, it estimates R_0 as an average regardless of whether the population is of human or host cells. It also lacks some uniqueness (Smith et al., 2011). To address the challenges of those methods, this study determined R_0 using three methods for comparative purposes: Sub-Sub section **4.1.4.1** next-generation matrix, **4.1.4.2** Survival Function and **4.1.4.3** constant term of the characteristic polynomial.

4.1.4.1 Using next generation matrix

Theorem 4: The basic reproduction number, $R_0 = \frac{(M+F)(K_1-S^0)\gamma_1}{K_1(M\beta+F\beta+ME+M\delta_1+F\delta_1+M\eta_1+F\eta_1)}$ by Next-generation method.

Proof

We employ Kermack and Diekmann's next generation matrix approach to get a basic reproduction number (Diekmann et al., 1990). Let new infections terms be

represented by non-negative matrix f and transfer of infections terms by non-singular matrix v, respectively.

Thus

$$f = \begin{bmatrix} r_1 I\left(1-\frac{N}{K_1}\right)+\frac{\tau_2 SV}{S+BV} \\ r_1 P\left(1-\frac{N}{K_1}\right) \\ r_1 C\left(1-\frac{N}{K_1}\right)\left(1-\frac{C}{K_4}\right) \\ r_1 V+\omega_1\eta_1 I+\omega_2\eta_2 P+\omega_3\eta_3 C\left(1-\frac{V}{K_2}\right) \end{bmatrix};$$

$$v = \begin{bmatrix} \beta I+\frac{EM}{F+M}I+\eta_2 I+\delta_1 I \\ -\beta I+\frac{\theta C P^2}{D^2+P^2}+\eta_2 P+\delta_1 P \\ \left(-\frac{\theta C P^2}{D^2+P^2}+\eta_3 C+\delta_1 C\right)\left(1-\frac{C}{K_4}\right) \\ \tau_1 SV+\frac{\epsilon LV}{L+K_4}+\delta_2 V \end{bmatrix}$$

At E^0point, Jacobian matrices of f and v were evaluated to find out matrices F and V respectively,

$$F = \begin{bmatrix} \left(1-\frac{S^0}{K_1}\right)\gamma_1 & 0 & 0 & \frac{-\beta S^0 V\tau_2}{S_2} \\ 0 & \left(1-\frac{S^0}{K_1}\right)\gamma_1 & 0 & 0 \\ 0 & 0 & \left(1-\frac{S^0}{K_1}\right)\gamma_1 & 0 \\ \eta_1\omega_1 & \eta_2\omega_2 & \eta_3\omega_3 & \gamma_2 \end{bmatrix};$$

$$V = \begin{bmatrix} \beta+\frac{EM}{F+M}+\delta_1+\eta_1 & 0 & 0 & 0 \\ -\beta & \delta_1+\eta_2 & 0 & 0 \\ 0 & 0 & \delta_1+\eta_3 & 0 \\ 0 & 0 & 0 & \frac{L^0\epsilon}{L^0+K_5}+\delta_2+\tau_1 S^0 V \end{bmatrix}$$

At E^0point, FV^{-1},was obtained as,

$$\begin{bmatrix} \frac{(1-\frac{S^0}{K_1})r_1}{\frac{MQ}{F+M}+\beta+\delta_1+\eta_1} & 0 & 0 & 0 \\ 0 & \frac{(1-\frac{S^0}{K_1})r_1}{\delta_1+\eta_2} & 0 & 0 \\ 0 & 0 & \frac{(1-\frac{S^0}{K_1})r_1}{\delta_1+\eta_3} & 0 \\ 0 & 0 & 0 & \frac{r_2}{\frac{L^0\epsilon}{L^0+K_5}+\delta_2+\tau_1 S^0 V} \end{bmatrix}$$

The four eigenvalues were;

$$\frac{(K_1-S^0)\gamma_1}{K_1(\delta_1+\eta_3)}, \frac{(K_1-S^0)\gamma_1}{K_1(\delta_1+\eta_2)}, \frac{(M+F)(K_1-S^0)\gamma_1}{K_1(M\beta+F\beta+ME+M\delta_1+F\delta_1+M\eta_1+F\eta_1)} \; and \; \frac{(L^0+K_4)\gamma_2}{\epsilon L^0+\delta_2 L^0+K_4\delta_2}$$

By inspection method(which was verified by numerical method too) the dominant eigenvalue represents the R_0 (Diekmann et al., 1990). Hence

$$R_0 = \frac{(M+F)(K_1-S^0)\gamma_1}{K_1(M\beta+F\beta+ME+M\delta_1+F\delta_1+M\eta_1+F\eta_1)}$$

4.1.4.2 Basic Reproduction Number by Survival Function

Theorem 5: The basic reproduction number

$$R_0 = \frac{r_1\left(1-\frac{N}{K_1}\right)+\frac{\tau_2 S^0 V}{S+BV}}{\beta+\frac{EM}{F+M}+\eta_1+\delta_1} + \frac{r_1\left(1-\frac{N}{K_1}\right)}{\frac{\theta CP}{D^2+P^2}+\eta_2+\delta_2} + \frac{r_1\left(1-\frac{N}{K_1}\right)}{\left((\eta_3+\delta_1)\left(1-\frac{C}{K_4}\right)\right)}$$

$$+\frac{(r_2 V+\omega_1\eta_1 I+\omega_2\eta_2 P+\omega_3\eta_3 C)(1-\frac{V}{K_2})}{\frac{\epsilon L^0}{L+K_4}+\delta_2+\tau_1 SV}$$

By the method proposed by (Shaw & Kennedy, 2021) where;

$N(0), S(0), V(0), P(0), C(0), I(0)\; and\; L(0)$ are assumed to be constant terms at the beginning of the epidemic. For numerical computation, in this study, we assumed those constant values to be the initial conditions of the model.

Proof

Evaluation of R_0 using the survival function method is considered to be a more accurate method**.** The survival function approach produces the average number of secondary basal cells infected by one infected basal cell in the same class, which is one of its advantages (Smith et al., 2011). It also takes into account the different attributes of the population, therefore, the basic reproduction number using the survival function is given by; R_0=$\int_0^\infty (k \times b \times p)dt$ where:k= rate at which an individual in that class causes an infection, b= probability at which an infected individual remains in the same class to cause an infection. p= probability that an infected case will enter that class (Shaw & Kennedy, 2021).

Considering the infectious classes (I, P, C, and V), and $\boldsymbol{N}, S, V, P, C, I \; and \; L$ are assumed to be constant terms at the beginning of the epidemic, evaluating R_0 of equations (2), (3), (4) and (5), the basic reproduction number was obtained by summing them (Smith et al., 2011) that is,

$$\left\{r_1\left(1-\frac{N}{K_1}\right)+\frac{\tau_2 SV}{S+BV}\right\}\int_0^\infty e^{-\left(\beta+\frac{EM}{F+M}+\eta_1+\delta_1\right)T_A}dT_A+\left\{r_1\left(1-\right.\right.$$

$$\left.\left.\frac{N}{K_1}\right)\right\}\int_0^\infty e^{-\left(\frac{\theta CP}{D^2+P^2}+\eta_2+\delta_2\right)T_A}dT_A+\left\{r_1\left(1-\frac{N}{K_1}\right)\right\}\int_0^\infty e^{-\left((\eta_3+\delta_1)\left(1-\frac{C}{K_4}\right)\right)T_A}dT_A+$$

$$\left\{(r_2V+\omega_1\eta_1 I+\omega_2\eta_2 P+\omega_3\eta_3 C)(1-\frac{V}{K_2})\right\}\int_0^\infty e^{-\left(\frac{\epsilon L}{L+K_4}+\delta_2+\tau_1 SV\right)T_A}dT_A$$

Integrating, $$\left\{r_1\left(1-\frac{N}{K_1}\right)+\frac{\tau_2 SV}{S+BV}\right\}\left[-\frac{e^{-\left(\beta+\frac{EM}{F+M}+\eta_1+\delta_1\right)T_A}}{\beta+\frac{EM}{F+M}+\eta_1+\delta_1}\right]_0^\infty+\left\{r_1\left(1-\right.\right.$$

$$\left.\left.\frac{N}{K_1}\right)\right\}\left[-\frac{e^{-\left(\frac{\theta CP}{D^2+P^2}+\eta_2+\delta_2\right)T_A}}{\frac{\theta CP}{D^2+P^2}+\eta_2+\delta_2}\right]_0^\infty+\left\{r_1\left(1-\frac{N}{K_1}\right)\right\}\left[-\frac{e^{-\left((\eta_3+\delta_1)\left(1-\frac{C}{K_4}\right)\right)T_A}}{\left((\eta_3+\delta_1)\left(1-\frac{C}{K_4}\right)\right)}\right]_0^\infty+\left\{(r_2V+\right.$$

$$\left.\omega_1\eta_1 I+\omega_2\eta_2 P+\omega_3\eta_3 C)(1-\frac{V}{K_2})\right\}\left[\frac{e^{-\left(\frac{\epsilon L}{L+K_4}+\delta_2+\tau_1 SV\right)T_A}}{\frac{\epsilon L}{L+K_4}+\delta_2+\tau_1 SV}\right]_0^\infty.$$

Putting the limits the basic reproduction number is obtained as:

$$\boldsymbol{R_0} = \frac{r_1\left(1-\frac{N}{K_1}\right)+\frac{\tau_2 S^0 V}{S+BV}}{\beta+\frac{EM}{F+M}+\eta_1+\delta_1} + \frac{r_1\left(1-\frac{N}{K_1}\right)}{\frac{\theta CP}{D^2+P^2}+\eta_2+\delta_2} + \frac{r_1\left(1-\frac{N}{K_1}\right)}{\left((\eta_3+\delta_1)\left(1-\frac{C}{K_4}\right)\right)}$$

$$+\frac{(r_2 V+\omega_1\eta_1 I+\omega_2\eta_2 P+\omega_3\eta_3 C)(1-\frac{V}{K_2})}{\frac{\epsilon L^0}{L+K_4}+\delta_2+\tau_1 SV}$$

4.1.4.3 Basic Reproduction number by evaluating the constant term of the characteristic polynomial.

Theorem 6: The basic reproduction number

$R_0 = \frac{(F+M)(S^0-K_1)^3(L^0+K_4)r_1^3 r_2}{K_1^3(F\beta+M(Q+\beta)+(F+M)(\delta_1+\eta_1))(\delta_1+\eta_2)(\delta_1+\eta_3)(L^0\epsilon+(L^0+K_4)(\delta_2+S\tau_1))}$ by method evaluating the constant term of the characteristic polynomial (Smith et al., 2011).

Proof

For comparison purposes, there is a need to determine the basic reproduction number using the constant term of a characteristic polynomial. When λ max = 0, the constant term of the characteristic polynomial will be zero (Smith et al., 2011). However, the reverse is not true, as the polynomial could have both zero and positive roots**.** The characteristic polynomial by next- generation matrix (FV^{-1}) is of the form $b_4\lambda^4 + b_3\lambda^3 + b_2\lambda^2 + b_1\lambda + b_0 = 0$, where the expressions of $b_4, b_3, b_2, b_1 \; and \; b_0$ are found in the appendix in section 4. The study (Smith et al., 2011) proposes the following conditions.

Let b_0 represent R_0, then b_0= 0 is a threshold if $b_j \geq 0$ for all j. Some sufficient conditions include; non-constant coefficients all being positive and $b_j \geq 0$ under the constraint b_0= 0 (so that the largest eigenvalue at b_0 = 0 is 0). Comparing this method to determining the biggest eigenvalue, it is much simpler to employ, although verifying that b_j= 0 requires that the greatest eigenvalue matches to can get complex for some models (Smith et al., 2011).

$R_0 = \frac{(F+M)(S^0-K_1)^3(L^0+K_4)r_1^3 r_2}{K_1^3(F\beta+M(Q+\beta)+(F+M)(\delta_1+\eta_1))(\delta_1+\eta_2)(\delta_1+\eta_3)(L^0\epsilon+(L^0+K_4)(\delta_2+S\tau_1))}$.

4.1.5 Endemic equilibrium

By setting the system of equations to zero and evaluating the state variables, the endemic equilibrium points would be in the form:

$$(EEP) = (S^*, I^*, P^*, C^*, V^*, L^*)$$

From; $\left\{r_1 C^* \left(1 - \frac{N}{K_1}\right) + \Theta \frac{C^* P^{*2}}{D^2 + P^{*2}} - \eta_3 C^* - \delta_1 C^*\right\}\left(1 - \frac{C^*}{K_4}\right) = 0$

It follows that; $C^* = K_4$

The endemic equilibrium point exists at $C^* = K_4$ and since the equations are highly non-linear, it was not tractable to solve them explicitly.

From; $r_1 P^* \left(1 - \frac{N}{K_1}\right) + \beta I^* - \Theta \frac{C^* P^{*2}}{D^2 + P^{*2}} - \eta_2 P^* - \delta_1 P^* = 0$

$$P^* = \frac{-C\theta K_1 \pm \sqrt{C^2\theta^2 K_1^2 - 4(\beta K_1 - N r_1 + K_1 r_1 - K_1\delta_1 - K_1\eta_2)(D^2\beta K_1 - D^2 N r_1 + D^2 K_1 r_1 - D^2 K_1\delta_1 - D^2 K_1\eta_2)}}{2(-\beta K_1 + N r_1 - K_1 r_1 + K_1\delta_1 + K_1\eta_2)}$$

From; $\{r_2 V^* + \omega_1\eta_1 I^* + \omega_2\eta_2 P^* + \omega_3\eta_3 C^*\}\left(1 - \frac{V^*}{K_2}\right) - \tau_1 S V - \epsilon \frac{L^*}{L^* + K_4} V^* - \delta_2 V^* = 0$

$$V^* = \frac{K_2\left(\frac{L\epsilon}{K_4} - r_2 + \frac{J\eta_1\omega_1}{K_2} + \frac{P\eta_2\omega_2}{K_2} + \frac{T\eta_3\omega_3}{K_2} + \sqrt{\frac{4r_2(J\eta_1\omega_1 + P\eta_2\omega_2 + T\eta_3\omega_3)}{K_2} + \left(-\frac{L\epsilon}{K_4} + r_2 - \frac{J\eta_1\omega_1}{K_2} - \frac{P\eta_2\omega_2}{K_2} - \frac{T\eta_3\omega_3}{K_2}\right)^2}\right)}{2r_2}$$

Substituting the value of $P^*, C^* \text{ and } V^*$ to;

$r_1 I^* \left(1 - \frac{N}{K_1}\right) + \frac{\tau_2 S^0 V}{S + BV^*} - \beta I^* - \frac{EM}{F+M} I^* - \eta_1 I^* - \delta_1 I^* > 0$ and solving for I^*, we get the value of $I^* = -\frac{\tau_2 M}{(S+BV)\left(-\frac{EM}{F+M} - \beta + \left(1 - \frac{X}{K_1}\right) r_1 - \delta_1 - \eta_1\right)}$

From $r_3 L^* \left(1 - \frac{L^*}{K_3}\right) - \alpha_1 L^* V^* - \delta_3$

$L^* = \frac{K_3(r_3 - V\delta_1 - \delta_3)}{r_3}$

Theorem 7: The necessary and sufficient conditions for existence are $R_0 > 1$, $\frac{dI}{dt} > 0, \frac{dP}{dt} > 0, \frac{dC}{dt} > 0 \text{ and } \frac{dV}{dt} > 0$ (Kilonzi et al., 2024).

4.1.6 Stability analysis

4.1.6.1 Local stability of disease-free equilibrium point

Theorem 2. The Disease Free Equilibrium of the system (1)-(6) is locally asymptomatic stable whenever $R_0 < 1$.

Proof:

The relative stability of the system can be determined by the Routh-Hurwitz criterion of stability without having to solve each equation.

Determining Jacobian Matrix of the system (1)-(6) at Disease Free Equilibrium is obtained;

$$[R_1 \quad R_2 \quad R_3 \quad R_4 \quad R_5 \quad R_6]^T$$

$$R_1 = \left[-\delta_1 - k_1 r_1 S^0(1-k_1 S^0) \quad \Omega_1 - k_1 r_1 S^0(1-k_1 S^0) \quad -k_1 r_1 S^0(1-k_1 S^0) \quad -k_1 r_1 S^0(1-k_1 S^0) \quad \frac{\tau_2 B}{S^0} \quad 0\right]$$

$$R_2 = \left[0 \quad (1-k_1 S^0) r_1 - \Omega_2 \quad 0 \quad 0 \quad -\frac{\tau_2 B}{S^0} \quad 0\right]$$

$$R_3 = [0 \quad \beta \quad (1-k_1 S^0) r_1 - \Omega_3 \quad 0 \quad 0 \quad 0]$$

$$R_4 = [0 \quad 0 \quad 0 \quad (1-k_1 S^0) r_1 - \Omega_4 \quad 0 \quad 0]$$

$$R_5 = \left[0 \quad \eta_1 \omega_1 \quad \eta_2 \omega_2 \quad \eta_3 \omega_3 \quad -\frac{\epsilon L^0}{L^0 + K_4} + r_2 - \delta_2 - \tau_1 S^0 \quad 0\right]$$

$$R_6 = [0 \quad 0 \quad 0 \quad 0 \quad -\alpha_1 L^0 \quad -\delta_3 - k_3 r_3 L^0(1-k_3 L^0)]$$

The characteristic polynomial is obtained as $a_0\lambda^6 + a_1\lambda^5 + a_2\lambda^4 + a_3\lambda^3 + a_4\lambda^2 + a_5\lambda + a_6 = 0$, where the expression $a_i, i = 1$ for the system (1)-(6) are in appendix section 2. The Routh table for the coefficients was also derived in the appendix in section 1.

From the characteristic polynomial, the values $a_2, a_4, a_6, b_1, c_1, d_1 \; and \; e_1$ are determined using Mathematica Software and expressed in terms of Ro. By Routh-Hurwitz Criteria for stability, the system (1) -(6) is locally asymptotically stable at DFE whenever $Ro < 1$ if and only if $a_2 > 0, a_4 > 0, a_6 > 0, b_1 > 0, c_1 > 0, d_1 >$

$0, e_1 > 0$ are satisfied and otherwise unstable (Mutua et al., 2022). The values of $a_2, a_4, a_6, b_1, c_1, d_1\ and\ e_1$ have been expressed in the appendix.

4.1.6.2 Global Stability of disease-free equilibrium point

The global stability of disease-free equilibrium is investigated using the Castillo-Chavez Metzler Matrix method. $\frac{dX}{dt} = F(X,Z)$; $\frac{dZ}{dt} = G(X,Z)$, $G(X,0) = 0$ Where; $X = (S,L)\epsilon R_2^+$ denote non-infectious cervical cancer compartments and $Z = (I,P,C,V)\epsilon\ R_4^+$ denote the infectious cervical cancer compartments $Eo = (X*,0)$ represents the disease-free equilibrium of the system if this point satisfies following conditions.

i. $\frac{dX}{dt} = (X,0)$, Where $X*$ is globally asymptotically stable.

ii. $\frac{dZ}{dt} = DzG(X,0)Z - G(X,Z) \geq 0$ for all X,$Z \in \Omega$, then we can conclude that Eo is locally asymptotically stable if the following theorems hold.

Theorem; The equilibrium point $Eo = (X*,0)$ of the system [1-6] is globally asymptotically stable if $R_0^* \leq 1$ and the conditions (i) and (ii) are satisfied, otherwise unstable. From equation (1) two vectors function $G(X, Z)$ and $F(X,Z)$, we consider systems $\frac{dX}{dt} = (X,0) = 0$ Letting $A = D_z G(X*,0)$, which is the Jacobian of $\hat{G}(X,Z)$ taken in (I, P, C, V) and evaluated at ($X*$,0) such that the matrix A is given by;

$$AZ = \begin{bmatrix} (\beta_1 S^0 - k_1)E + \eta_1\beta_1 S^0 I + \eta_2\beta_1 S^0 T + \eta_3\beta_1 S^0 C \\ \rho E - k_2 I \\ \omega I - k_3 T \\ \gamma I + \alpha T - k_4 C \end{bmatrix}$$

$$G(X,Z) = \begin{bmatrix} (\lambda_1 + \lambda_2)S - k_1 E \\ \rho E - k_2 I \\ \omega I - k_3 T \\ \gamma I + \alpha T - k_4 C \end{bmatrix}$$

But $$G^{\wedge}(X,Z) = AZ - G(X,Z)$$

hence,
$$G^{\wedge}(X,Z) = \begin{bmatrix} G^{\wedge}_1(X,Y) \\ G^{\wedge}_2(X,Y) \\ G^{\wedge}_3(X,Y) \\ G^{\wedge}_4(X,Y) \end{bmatrix} = \begin{bmatrix} (\beta_1(E+\eta_1 I+\eta_2 T+\eta_3 C)(S^0-S)-\lambda_2 S \\ 0 \\ 0 \\ 0 \end{bmatrix}$$

Thus, if then the disease-free equilibrium (E^0) is globally stable and unstable otherwise. The susceptible is bounded as, $S \le S^0$.Thus, DFE, E^0 is globally asymptomatically stable if and only if $(\beta_1(E+\eta_1 I+\eta_2 T+\eta_3 C)(S^0-S) \ge \lambda_2 S$ (Kilonzi et al., 2024), (Ochwach et al., 2022), (Mutua et al., 2022).

4.1.6.3 Global Stability Analysis of Endemic Equilibrium Point

Lyapunov functions are mathematical tools used to study the stability of dynamical systems. Different Lyapunov functions are employed for global stability analysis such as; quadratic, non-quadratic, radial basis functions, composite and piecewise Lyapunov functions. This study adopted composite Lyapunov function.

$$L = \sum b_i(x_i - x_i^* \ln x_i)$$

The function L is said to be positive definite if it satisfies the following conditions:

i) Strict positivity: $L > 0$ for all $x \neq 0$.

ii) Zero at origin: $L(0) = 0$.

Where b_i the constant is selected such that $b_i > 0$, x_i is the population of the i^{th} compartment and $x_i^*$is the endemic equilibrium point.

$$L = b_1(S - S^* \ln S) + b_2(I - I^* \ln I) + b_3(P - P^* \ln P) + b_4(C - C^* \ln C) + b_5(V - V^* \ln V) + b_3(L - L^* \ln L)$$

$$\frac{dL}{dt} = b_1\left(1 - \frac{S^*}{S}\right)\frac{dS}{dt} + b_2\left(1 - \frac{I^*}{I}\right)\frac{dI}{dt} + b_3\left(1 - \frac{C^*}{C}\right)\frac{dC}{dt} + b_4\left(1 - \frac{P^*}{P}\right)\frac{dP}{dt} + b_5\left(1 - \frac{V^*}{V}\right)\frac{dV}{dt} + b_6\left(1 - \frac{L^*}{L}\right)\frac{dL}{dt}$$

$$\frac{dL}{dt} = b_1\left(1-\frac{S^*}{S}\right)\left\{r_1 S(1-k_1 N) - \frac{\tau_2 S}{S+BV} + \Omega_1 I - \delta_1 S\right\}$$
$$+ b_2\left(1-\frac{I^*}{I}\right)\left\{r_1 I(1-k_1 N) + \frac{\tau_2 S}{S+BV} - \Omega_2 I\right\}$$
$$+ b_3\left(1-\frac{C^*}{C}\right)\left\{\left\{r_1 C(1-k_1 N) + \theta\frac{CP^2}{D^2+P^2} - \Omega_4 C\right\}(1-k_4 C)\right\}$$
$$+ b_4\left(1-\frac{P^*}{P}\right)\left\{r_1 P(1-k_1 N) + \beta I - \theta\frac{CP^2}{D^2+P^2} - \Omega_3 P\right\}$$
$$+ b_5\left(1-\frac{V^*}{V}\right)\left\{\{r_2 V + \omega_1\eta_1 I + \omega_2\eta_2 P + \omega_3\eta_3 C\}(1-k_2 V)\right.$$
$$\left. - \tau_1 SV - \epsilon\frac{L}{L+K_4}V - \delta_2 V\right\}$$
$$+ b_6\left(1-\frac{L^*}{L}\right)\{r_3 L(1-k_3 L) - \alpha_1 LV - \delta_3 L\}$$

After solving we obtain the value of X and Y as follows.

$$X = \quad b_1 r_1 S + b_1\Omega_1 I + bS^* r_1 K_1 N + \frac{bS^*\tau_2}{S+BV} + bS^*\delta_1 + b_2 r_1 I + b_2\tau_2 S + b_2 I^* K_1 N +$$
$$b_2 I^*\Omega_2 + b_3 r_1 C + b_3\frac{\theta CP^2}{D^2+P^2} + b_3 r_1 C^2 K_1 K_4 N + b_3\Omega_4 C^2 K_4 + b_3 K_1 N C^* + b_3\Omega_4 C^* +$$
$$b_3 K_4 C C^* r_1 + b_3\frac{\theta C^* CP^2 K_4}{D^2+P^2} + b_4 r_1 P + b_4\beta\mathrm{I} + b_4 r_1 P K_1 N K_4 C + b_4\frac{\theta CP^2}{D^2+P^2}K_4 C +$$
$$b_4\Omega_4 C^2 K_4 + b_4\frac{P^*}{P}(r_1 P K_1 N + \frac{\theta CP^2}{D^2+P^2} + \Omega_4 C + r_1 P K_4 C + \beta I C K_4 + b_5(r_2 V +$$
$$\omega_1\eta_1 I + \omega_2\eta_2 P + \omega_3\eta_3 C + \omega_2\eta_2 P K_2 V + b_5\frac{V^*}{V}(r_2 K_2 V^2 +$$
$$\omega_1\eta_1 I K_2 V + \omega_3\eta_3 C K_2 V + \tau_1 SV + \frac{\epsilon LV}{L+K_4} + \delta_2 V) + b_6 r_3 L + b_6\frac{L^*}{L}(r_3 L^2 K_3 + \alpha_1 LV +$$
$$\delta_3 L)$$

$$Y = -br_1 SK_1 N - \frac{bS\tau_2}{S+BV} - bS\delta_1 - bS^* r_1 - \frac{bS^*\Omega_1 I}{S} - b_2 r_1 I K_1 N - b_2\Omega_2 I -$$
$$b_2 I^* r_1 - b_2\frac{I^*}{I}\frac{S\tau_2}{S+BV} - b_3 r_1 C K_1 N - b_3\Omega_4\mathrm{C} - b_3 r_1 C^2 K_4 - b_3\frac{\theta C^2 P^2 K_4}{D^2+P^2} - b_3 C^* -$$
$$b_3\frac{\theta C^* P^2}{D^2+P^2} - b_3 C^*\Omega_4 C K_4 - b_3 C^*\mathrm{K_1} C K_4 r_1 - b_4(r_1 P K_1 N + \frac{\theta CP^2}{D^2+P^2} + \Omega_4 C + r_1 P K_4 C +$$
$$\beta\mathrm{I}K_4 C) - b_4\frac{P^*}{P}(r_1 P + \beta\mathrm{I} + r_1 P K_1 N K_4 C + \frac{\theta CP^2}{D^2+P^2}K_4 C) - b_5(r_2 K_2 V^2 +$$
$$\omega_1\eta_1 I K_2 V + \omega_3\eta_3 C K_2 V + \tau_1 SV + \frac{\epsilon LV}{L+K_4} + \delta_2 V) - b_5\frac{V^*}{V}(r_2 V + \omega_1\eta_1 I + \omega_2\eta_2 P +$$
$$\omega_3\eta_3 C + \omega_2\eta_2 P K_2 V) - b_6(r_3 L^2 K_3 + \alpha_1 LV + \delta_3 L) - b_6 L^* r_3$$

By inspection method $X > Y$, therefore this result shows that cervical cancer would persist whenever $X > Y$ irrespective of the initial conditions, and if $Y > X$ regardless of the starting settings, the sickness will eventually disappear. It follows that the global stability for EEP for the system exists for those without underlying medical issues (Kilonzi et al., 2024).

4.1.7. Bifurcation Analysis

Most mathematical models often undergo bifurcation which makes the control of most diseases difficult. Utilizing the center manifold theory, the likelihood of population hopf bifurcation was investigated. The renaming of variables is done simply by letting, $S = x_1, I = x_{2,} P = x_3, C = x_{4,} V = x_{5,} L = x_6$

Using vector notation;

$x = x_1, x_{2,} x_{3,} x_{4,} x_{5,} x_6$

The system (1)-(6) is written as,

$\frac{dx}{dt} = F(x)$ where $F = (f_1, f_{2,} f_3, f_4, f_5, f_6)^T$, It follows that:

$$\frac{d_{x_1}}{dt} = p_1 = r_1 f_1 \left(1 - \frac{N}{K_1}\right) - \frac{\tau_2 f_1 f_5}{f_1 + B f_5} + \frac{EM}{F+M} f_2 - \delta_1 f_1$$

$$\frac{dx_2}{dt} = p_2 = r_1 f_2 \left(1 - \frac{N}{K_1}\right) + \frac{\tau_2 f_1 f_5}{f_1 + B f_5} - \beta f_2 - \frac{EM}{F+M} f_2 - \eta_1 f_2 - \delta_1 f_2$$

$$\frac{dx_3}{dt} = p_3 = r_1 f_3 \left(1 - \frac{N}{K_1}\right) + \beta f_2 - \theta \frac{f_4 {f_3}^2}{D^2 + {f_3}^2} - \eta_2 f_3 - \delta_1 f_3.$$

$$\frac{dx_4}{dt} = p_4 = \left\{r_1 f_4 \left(1 - \frac{N}{K_1}\right) + \theta \frac{f_4 {f_3}^2}{D^2 + {f_3}^2} - \eta_3 f_4 - \delta_1 f_4\right\} \left(1 - \frac{f_4}{K_4}\right).$$

$$\frac{dx_5}{dt} = p_5 = \{r_2 f_5 + \omega_1 \eta_1 f_2 + \omega_2 \eta_2 f_3 + \omega_3 \eta_3 f_4\} \left(1 - \frac{f_5}{K_2}\right) - \tau_1 f_1 f_5 - \epsilon \frac{f_6}{f_6 + K_4} f_5 - \delta_2 f_5.$$

$$\frac{dx_6}{dt} = p_6 = r_3 f_6 \left(1 - \frac{f_6}{K_3}\right) - \alpha_1 f_6 f_5 - \delta_3 f_6.$$

Jacobian solved at DFE,

$E^0 = (S^0, I^0, P^0, C^0, V^0, L^0) = \left(\frac{K_1(r_1-\delta_1)}{r_1}, 0,0,0,0, \frac{K_3}{r_3}(r_3-\delta_3)\right)$, in a case, where $R_0^* = 1$ and further, suppose that $r_1 = r_1^*$ is a bifurcation parameter, then solving for r_1^* from $R_0^* = 1$ we get,

$$r_1^* = \frac{K_1(MQ + F\beta + M\beta + F\delta_1 + M\delta_1 + F\eta_1 + M\eta_1)}{(F+M)(K_1 - S^0)}$$

Gives

$$\begin{bmatrix} A_1 & A_2 \\ A_3 & A_4 \end{bmatrix}$$

Where;

A_1

$$= \begin{bmatrix} (1-\frac{S^0}{K_1})r_1^* - \frac{r_1^* S^0}{K_1} - \delta_1 & \frac{ME}{F+M} - \frac{r_1^* S^0}{K_1} & -\frac{r_1^* S^0}{K_1} \\ 0 & -\frac{ME}{F+M} - \beta + (1-\frac{S^0}{K_1})r_1^* - \delta_1 - \eta_1 & 0 \\ 0 & \beta & (1-\frac{S^0}{K_1})r_1^* - \delta_1 - \eta_2 \end{bmatrix}$$

It can easily be shown that, Jacobian of the system

$$A_2 = \begin{bmatrix} -\frac{r_1^* S^0}{K_1} & \frac{\tau_2 B}{S^0} & 0 \\ 0 & -\frac{\tau_2 B}{S^0} & 0 \\ 0 & 0 & 0 \end{bmatrix} \qquad A_3 = \begin{bmatrix} 0 & 0 & 0 \\ 0 & \eta_1\omega_1 & \eta_2\omega_2 \\ 0 & 0 & 0 \end{bmatrix}$$

$$A_4 = \begin{bmatrix} (1-\frac{S^0}{K_1})r_1^* - \delta_1 - \eta_3 & 0 & 0 \\ \eta_3\omega_3 & \frac{\epsilon L^0}{L^0+K_4} + r_2 - \delta_2 - \tau_1 S^0 & 0 \\ 0 & -\alpha_1 L^0 & (1-\frac{L^0}{K_3})r_3 - \frac{r_3 L^0}{K_3} - \delta_3 \end{bmatrix}$$

It has been proved that at least one of the eigenvalues of the matrix is a simple zero eigenvalue (Mutua et al., 2022). Therefore, the bifurcation of the system can be evaluated using the Castillo-Chavez theorem.

Let $u = (u_1, u_{2,} u_3, u_4, u_5, u_6)^T$ be the right eigenvector and $v = (v_1, v_3, v_4, v_5, v_6)^T$ be the left eigenvector linked with zero eigenvalues of the Jacobian matrix near $r_1 = r_1^*$, of the system.

Solving the system of the equations, we obtain;

$$u_1 = 0 \ , \ u_2 = \frac{u_3\beta - u_5(\eta_1\omega_1)}{\Omega_1+\beta+(S^0k_1-1)-\delta_1-\eta_1} \ , \ u_3 = \frac{-u_5(\eta_3\omega_3)}{(1-S^0k_1)r_1-\eta_3} \ , \ u_4 = \frac{-u_5(\eta_3\omega_3)}{(1-S^0k_1)r_1-\eta_4}$$

$$u_5 = \frac{u_2-\frac{\tau_2 B}{S^0}+u_6\alpha_1L^0}{\frac{\epsilon L^0}{L^0+k_4}+r_2-\delta_2-\tau_1S^0} = \frac{u_2-\frac{\tau_2 B}{S^0}}{\frac{\epsilon L^0}{L^0+k_4}+r_2-\delta_2-\tau_1S^0} \ , \ u_6 = 0$$

$$v_1 = \frac{-(\eta_1-r_1S^0k_1)v_2+v_3r_1S^0k_1-r_1S^0k_1v_4+v_5\frac{\tau_2 B}{S^0}}{(1-S^0k_1)r_1-r_1S^0k_1-\delta_1} = \frac{v_3r_1S^0k_1+v_5\frac{\tau_2 B}{S^0}}{(1-S^0k_1)r_1-r_1S^0k_1-\delta_1} \ , \ v_2 = 0$$

$$v_3 = \frac{\left((S^0k_1-1)r_1+\eta_{1+\delta_1}+\Omega_1+\beta\right)v_2+v_5\frac{\tau_2 B}{S^0}}{(1-S^0k_1)r_1-\eta_3} = \frac{v_5\frac{\tau_2 B}{S^0}}{(1-S^0k_1)r_1-\eta_3} \quad , \quad v_4 = 0, \quad v_5 = \frac{-(\eta_2\omega_2)v_3-(\eta_3\omega_3)v_4}{\frac{\varepsilon L^0}{K_4+L^0}+r_2-\delta_2-\tau_1S^0} = \frac{-(\eta_2\omega_2)v_3}{\frac{\varepsilon L^0}{K_4+L^0}+r_2-\delta_2-\tau_1S^0} \ , \ v_6 = \frac{v_5\alpha_1L}{((1-L^0k_1)r_3-\frac{r_3L^0}{k_3}-\delta_3)} \ .$$

Let $p_k$be the kth component of p and

$$a = \sum_{k,ij=1}^{n} v_k u_i u_j \frac{\partial^2 p_k}{\partial f_i \partial f_j}(0,0) \ \text{ and } \ b = \sum_{k,ij=1}^{n} v_k u_i \frac{\partial^2 p_k}{\partial f_i \partial r_1^*}(0,0)$$

then the signs of a and b completely dictate the local dynamics of the system around the equilibrium point (0,0) (Gitonga, 2017).

On evaluating the values of a and b which are found in the appendix in section 3, we conclude that since, $a < 0$ and $b < 0$, when $r_1^* < 0$ with $|r_1^*| \ll 1, (0,0)$ is unstable; when $0 < r_1^* \ll 1, (0,0)$ is then there is a positive unstable equilibrium and it is asymptotically stable.

4.2 Parameters Estimation

Table 3: Parameters Estimation

Parameter	Value	Reference
r_1	0.8506	(Ma & Thibodeaux, 2023)
r_2	0.011	Estimated
r_3	0.902	Estimated
K_1	10,000,000	Estimated
K_2	100,000	Estimated
K_3	50,000	Estimated
K_4	6,500,000	Estimated
τ_2	0.000001	(Chakraborty et al., 2019)
β	0.0082	(Ndii, 2020)
θ	0.01	(Ma & Thibodeaux, 2023)
$\eta 1 = \eta 2 = \eta 3$	0.005	(Ma & Thibodeaux, 2023)
δ_1	0.0048	(Mondaini et al., 2021)
δ_2	0.0021	(Mondaini et al., 2021)
δ_3	0.0005	Estimated
D	10^5	(Erwin, 2017)
$\omega_1 = \omega_2 = \omega_3$	1000	(Verma et al., 2017)
M	0.00003333	(Mondaini et al., 2021)
α_1	0.0002	Estimated
ϵ	0.90005	Estimated
τ_1	0.0005	Estimated

Table 3: Estimation of parameters

4.3 Numerical Simulation

MATLAB2019a is applied in numerical simulation to show the dynamic behavior of the non-linear ODE in the system (1)–(6). With the initial conditions and parameter values, the simulations are executed (taken from the literature review and graphically depicted) in Table 3.

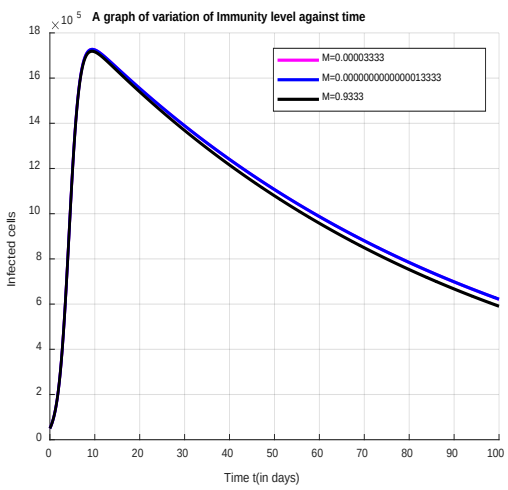

Figure 3: A graph of variation of immunity level against time.

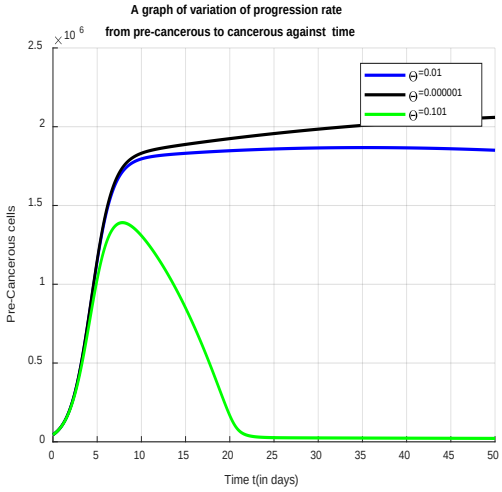

Figure 5: A graph of variation of progression rate from precancerous cells to cancerous against time

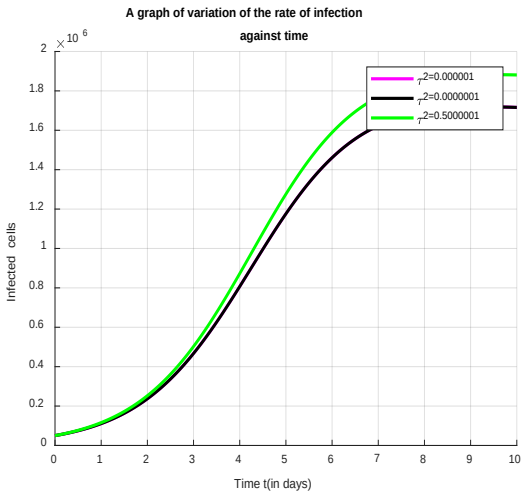

Figure 4: A graph of variation of the rate of infection against time

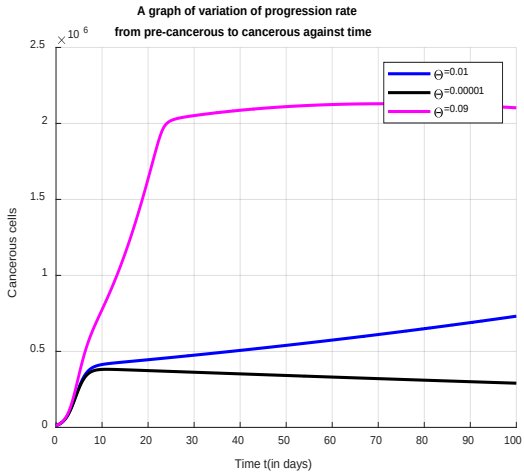

Figure 6: A graph of variation of progression rate from precancerous to cancerous against time

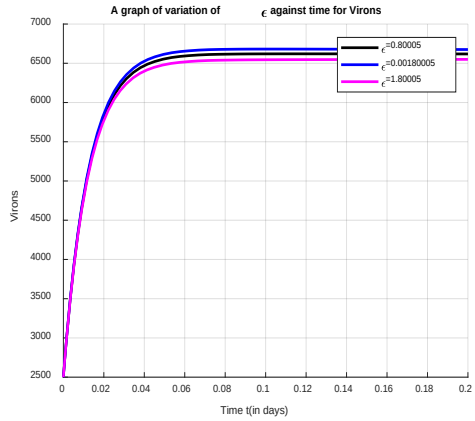

Figure 7: A graph of variation of ϵ against time for virons

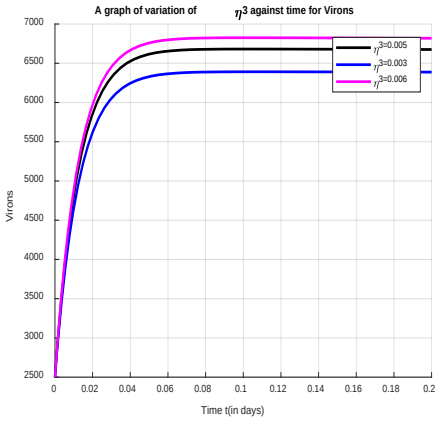

Figure 10: A graph of variation of η3 against time for virons

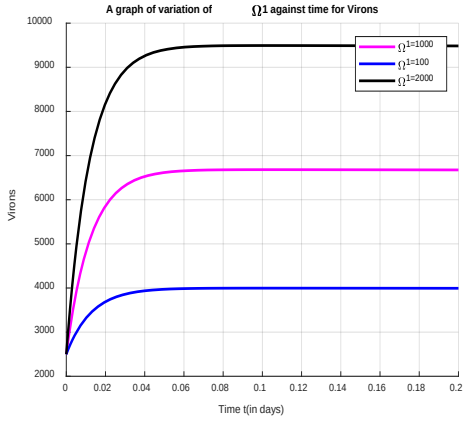

Figure 8: A graph of variation of Ω1 against time for virons

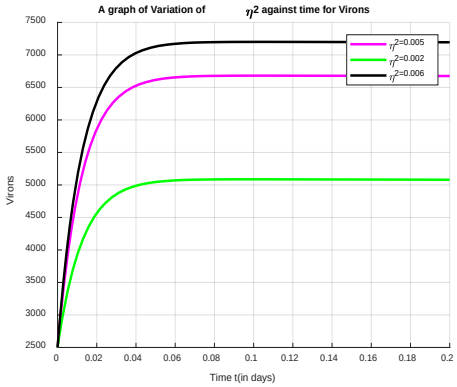

Figure 11: A graph of variation of η2 against time for virons

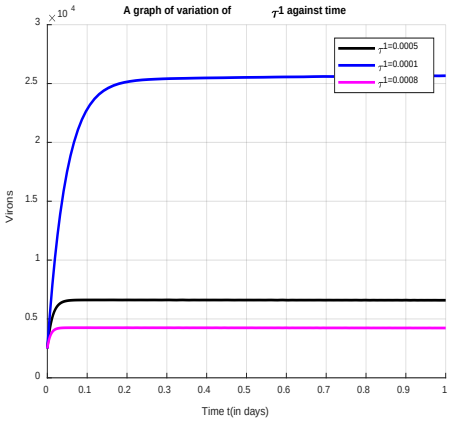

Figure 9: A graph of variation of r1 against time

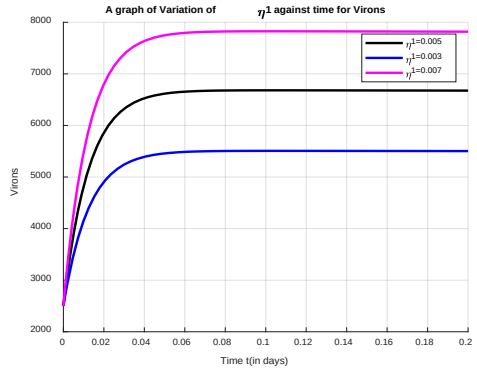

Figure 12: A graph of variation of η1 against time for virons

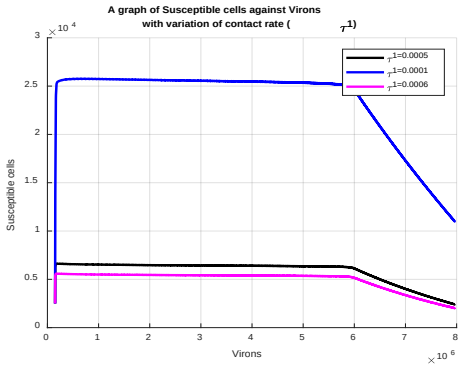

Figure 14: A graph of susceptible cells against virons with variation contact rate (τ1)

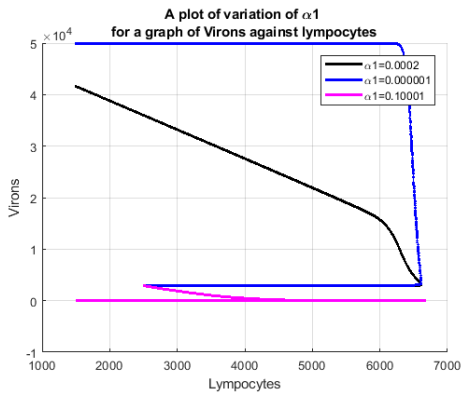

Figure 13: A plot of variation of α1 for a graph of virons against lymphocytes

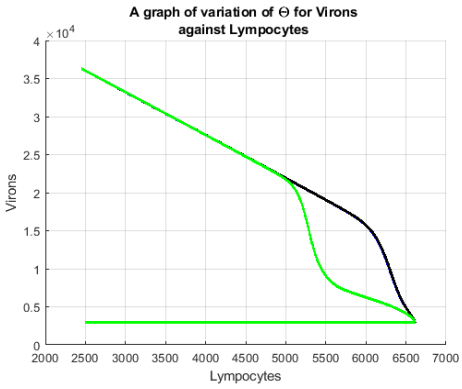

Figure 15: A graph of variation of θ virons against lymphocytes

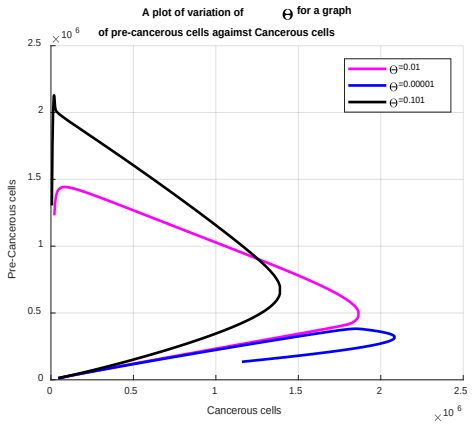

Figure 16: A graph of variation of θ for a graph of precancerous cells against cancerous cells

The graphs obtained from simulations are interpreted as follows.

The immunity level for the infected cells varied from M=0.0000333 to M= 0.000000000000001333 and M=0.9333 while the other parameters remained unchanged. Figure 3 shows that increasing the immunity level reduces the number of infected cells. This indicates that eating a balanced diet can boost the immunity level which fights the virus reducing the number of infected cells.

The infection rate for the infected cells was varied from $\gamma_{2=}$ 0.000001 to $\gamma_{2=}$0.5000001 while the other parameters were held constant. From figure 4 suggests that the number of infected cells grew in proportion to the increase in infection rate.

The Progression rate from Precancerous cells to Cancerous cells varied from θ=0.000001 to θ=0.101 while the other parameters were held constant. Figure 5 shows that when the progression rate was decreased it increased the pre-cancerous cells while when it was increased it significantly reduced the number of pre-cancerous cells.

The rate at which precancerous cells transform into cancerous ones was varied for Cancerous cells while the other parameters were held constant. The results as represented by Figure 5 indicate that when the rate was reduced it decreased the number of cancerous cells while when it was increased, the population of cancerous cells increased.

4.3 Sensitivity analysis of the model

The relationship below provides the sensitivity index of the model parameter;

$$S_X^{R_o} = \frac{\partial R_o}{\partial X} * \frac{X}{R_o}$$

Sensitivity analysis for the whole model is as follows.

Table 4: Table of sensitivity indices

Parameter	**Next Generation Matrix.**	**Survival Function.**	**Constant term of the characteristic polynomial.**
F	0.993351	0.0000346813344295621	0.993351
M	-0.99463	-0.000034681334429562096	-0.99463
K_1	-0.0000176205	0.026674154887992983	-0.000158879
r_1	1	0.9879380508173314	3
r_2	0	$5.883416249394072 \times 10^{-7}$	1
B	-1.05469×10^{-10}	$-0.000092123992392037 86$	-1.05469×10^{-10}
δ_1	6.17395×10^{-6}	-0.22125138109693612	-0.979586
δ_2	0	-0.12494859329913026	0.00799353
η_1	6.43119×10^{-6}	-0.047374582684402054	6.43119×10^{-10}
η_2	0	-0.29268294620149876	-0.510204
η_3	0	-0.1764099056748374	-0.510204
S	-176.208	-0.011490780279154997	-529.625
E	1	0	-1
L	0	0	0.00135933
K_4	0	-0.0006712604976524636	-6.36864×10^{-10}
ϵ	0	$-2.188287319016677 \times 10^{-11}$	6.36864×10^{-10}
τ_1	0	-0.011499992678394202	-1.00799
I	0	0.005348560226721884	0
ω_3	0	0.001337140056680471	0
ω_2	0	0.004813704204049696	0
ω_1	0	0.005348560226721884	0

K_2	0	0.00029487161100197416	0
D	0	0.04629077249233771	0
P	0	−0.01364474132726996	0
C	0	−0.025823926384812002	0
θ	0	−0.027832326961018047	0
E	0	−0.00003491252020486956	0
β	0	−0.08646595437424326	0
V	0	−0.011241531993419006	0
N	0	−0.026674154887992983	0

Table 4: Sensitivity indices

From the sensitivity indices table above, r_1 is the most positive parameter implying that it is directly related to the dynamics of high-risk HPV to cervical cancer. To reduce the risk of cervical cancer r_1 should be decreased while, S being the most negative means that it is inversely related to the cervical cancer and HPV dynamic. Increasing the value of S reduces the risk of the disease.

CHAPTER FIVE

DISCUSSION, CONCLUSION AND RECOMMENDATIONS

5.1 Discussion and Conclusion

In the presence of immunity and functional responses, this work aimed to construct an in-host density-dependent deterministic model for the dynamics of basal cells, virions, and lymphocytes and their consequences for cervical cancer. The general (SIVPC) model by (Chakraborty, Li, et al., 2019) was adjusted for our investigation to include the maximum number of malignant cells that can result in a patient's death. A system of six first-order non-linear ordinary differential equations that explain the dynamics of HPV to cervical cancer helped to achieve this goal in section 2. The survival function, method of characteristic polynomial, next-generation matrix, positivity and boundedness of the solution, equilibrium points, and basic reproduction number were employed in this work to investigate the behavior of the deterministic model; the local stability of the DFE was ascertained using the Routh-Hurwitz criteria for stability, and the global stability of the EEP was ascertained using the Castillo-Chavez approach.

The analysis revealed several important findings regarding the dynamics of the model. The Disease-Free Equilibrium (DFE) was found to persist even in the absence of the disease. Additionally, the model was well-bounded and remained within the positive region, indicating biologically feasible solutions. The presence of an endemic equilibrium point occurred when $R_0 > 1$, and the local stability of the DFE was determined to be unstable when $R_0^* > 1$, but locally asymptotically stable when $R_0^* < 1$. Furthermore, when $R_0 > 1$, the global stability of the endemic equilibrium point (EEP) was asymptotically stable.

Further examination of the simplified system, based on equations (1) to (6), showed that the global stability of the Disease-Free Equilibrium (DFE) was also asymptotically stable if $R_0^* < 1$. The absence of backward bifurcation indicated that it is feasible to completely eradicate cervical cancer under the right conditions. The basic reproduction number was calculated to be $-7.2485210 \times 10^{-6}$, and this value was used to simulate the model's dynamics.

It was observed that increasing the parameter $\gamma_2$led to a higher number of infected cells, thereby elevating the risk of cervical cancer. Conversely, reducing the parameter M, which might represent immune strength, decreased the number of infected cells, underscoring the importance of a balanced diet for boosting immunity. Additionally, the parameter θ had the most direct impact on patient outcomes. The model estimated that a patient could die within 10 days when $\theta = 0.01$, but could survive up to 20 days when $\theta = 0.09$.

Bifurcation analyses were also produced. Additionally, sensitivity indices for the model's system were calculated using the next-generation matrix, survival function, and characteristic polynomial, depending on the reproduction number. Also, sensitivity indices for the system of the model was performed based on the reproduction number using three methods which are next-generation matrix, survival function, and characteristic polynomial.

The model suggests a proportion of 75% of cancerous cells that can lead to the death of a cervical cancer patient however, future studies should focus to obtaining the real data for the proportion of cancerous cells that can lead to the death of a patient.

5.2 Recommendations

Human Papillomavirus is a significant risk factor for the emergence of cervical cancer. Therefore, it is crucial to take action to stop the spread of this virus hence the need to model HPV dynamics to cervical cancer more. This study recommends longitudinal studies tracking HPV infection progression in patients to improve parameter estimation, incorporate more detailed immune response dynamics, including the role of immune cells, develop more personalized models based on individual patient data to predict cancer progression more accurately and finally model the impact of interventions such as vaccination, screening, and treatment on HPV dynamics and cancer progression.

REFERENCES

Afolabi, M. A., Adewoye, K. S., Folorunso, A. I., & Omoloye, M. A. (2021). *A Mathematical Model on Transmission Dynamics of Meningococcal Meningitis*. *4*(10), 59–66.

Akgül, A., Ahmed, N., Raza, A., Iqbal, Z., Rafiq, M., Rehman, M. A., & Baleanu, D. (2021). A Fractal Fractional Model for Cervical Cancer Due to Human Papillomavirus Infection. *Fractals*, *29*(5), 1–11.

Asih, T. S. N., Lenhart, S., Wise, S., Aryati, L., Adi-Kusumo, F., Hardianti, M. S., & Forde, J. (2016). The Dynamics of HPV Infection and Cervical Cancer Cells. *Bulletin of Mathematical Biology*, *78*(1), 4–20.

Asih, T. S. N., Widodo, Aryati, L., & Kusumo, F. A. (2019). Cusp Bifurcation on Cervical Cancer Mathematical Model. *Journal of Physics: Conference Series*, *1321*(2).

Ault, K. A. (2006). Epidemiology and Natural History of Human Papillomavirus Infections in the Female Genital Tract. *Infectious Diseases in Obstetrics and Gynecology*, *2006*(Figure 1), 1–5.

Belew, B., & Melese, D. (2022). Modeling and Analysis of Predator-Prey Model with Fear Effect in Prey and Hunting Cooperation among Predators and Harvesting. *Journal of Applied Mathematics*, *2022*.

Bershadsky, M., Chirkov, M., Domoshnitsky, A., Rusakov, S., & Volinsky, I. (2019). Distributed Control and the Lyapunov Characteristic Exponents in the Model of Infectious Diseases. *Complexity*, *2019*, 71–73.

Chakraborty, S., Cao, X., Bhattyacharya, S., & Roy, P. K. (2019). The Role of HPV on Cervical Cancer with Several Functional Response: a Control Based Comparative Study. *Computational Mathematics and Modeling*, *30*(4), 439–453.

Chakraborty, S., Debbouche, A., & Roy, P. K. (2020). A Mathematical Modelling for Treatment of HPV Associated Cervical Cancer: NK and Effector T cell Based Control Study. *Nonlinear Studies*, *27*(2), 325–336.

Chakraborty, S., Li, X. Z., & Roy, P. K. (2019). How can HPV-Induced Cervical Cancer be Controlled by a Combination of Drug Therapy? A mathematical study. *International Journal of Biomathematics*, *12*(6).

Diekmann, O., Heesterbeek, J. A. P., & Metz, J. A. J. (1990). On the Definition and the Computation of the Basic Reproduction Ratio R0 in Models for Infectious Diseases in Heterogeneous Populations. *Journal of Mathematical Biology*, *28*(4), 365–382.

Engida Sado, A. (2019). Mathematical Modeling of Cervical Cancer with HPV Transmission and Vaccination. *Science Journal of Applied Mathematics and Statistics*, *7*(2), 21.

Gitonga, N. C. (2017). *Modeling Childhood Pneumonia and Its Implications Regarding Its Control Using Kenyan Data*. 1–120.

Gurmu, E. D., & Koya, P. R. (2019). *Impact of Chemotherapy Treatment on SITR*

Compartmentalization and Modeling of Human Papilloma Virus. *15*(3), 17–29.

Huppert, A., & Katriel, G. (2013). Mathematical Modeling and Prediction in Infectious Disease epidemiology. *Clinical Microbiology and Infection*, *19*(11), 999–1005.

Kaur, A., Sharma, B., Kukreja, V., & Malik, V. (2022). A Mathematical Model of Cervical Cancer using Causal Analysis. *AIP Conference Proceedings*, *2357*(May).

Kessler, T. A. (2017). Cervical Cancer: Prevention and Early Detection. *Seminars in Oncology Nursing*, *33*(2), 172–183.

Kilonzi, J. S., Ngari, C. G., & Karanja, S. (2024). *Modeling The Impact of Screening, Treatment and Underlying Health Conditions on Dynamics of Covid-19*. *January 2023*.

Kivuti-bitok, L. W., Pokhariyal, G. P., Mcdonnell, G., & Abdul, R. (2015). *A Mathematical Model of Cervical Cancer in Kenya*. *4*(2), 458–465.

Krakauer, J. W. (2009). Progress in Motor Control. *Learning*, *629*(585), 405–421.

Kumar, A., & Nilam. (2019). Dynamical Model of Epidemic Along with Time Delay; Holling Type II Incidence Rate and Monod–Haldane Type Treatment Rate. *Differential Equations and Dynamical Systems*, *27*(1–3), 299–312.

LaVigne, K., & Leitao, M. M. (2019). Cervical cancer prevention. *Fundamentals of Cancer Prevention: Fourth Edition*, 629–652.

Mondaini, R. P., Lectures, C., & Janeiro, R. De. (2021). Trends in Biomathematics: Chaos and Control in Epidemics, Ecosystems, and Cells. In *Trends in Biomathematics: Chaos and Control in Epidemics, Ecosystems, and Cells*.

Mutua, G. K., Ngari, C. G., Muthuri, G. G., & Kitavi, D. M. (2022). Mathematical Modeling and Simulating of Helicobacter Pylori Treatment and Transmission Implications on Stomach Cancer Dynamics. *Communications in Mathematical Biology and Neuroscience*, *2022*, 1–29.

Ndii, M. Z. (2020). *Mathematical Model of Cervical Cancer Treatment Using Chemotherapy Drug*. *February*, 10–16.

Norton, J. P. (2008). Algebraic Sensitivity Analysis of Environmental Models. *Environmental Modelling and Software*, *23*(8), 963–972.

Ochwach, J., Okongo, M. O., & Ngari, C. (2022). *Mathematical Modelling of Cholera Incorporating the Dynamics of the Induced Achlorhydria Condition and Treatment*. *November*.

Online, P., & Ezzati, P. M. (2020). *Health Policy NCD Countdown 2030 : pathways to achieving Sustainable Development Goal target 3 . 4*. *396*.

Pongsumpun, P. (2012a). *Mathematical Model of Cervical Cancer due to Human Papillomavirus Infection*. 157–161.

Pongsumpun, P. (2012b). *Mathematical Model of Cervical Cancer due to Human*

Papillomavirus Infection. *January*, 157–161.

Ryser, M. D., Myers, E. R., & Durrett, R. (2015). HPV Clearance and the Neglected Role of Stochasticity. *PLoS Computational Biology*, *11*(3), 1–17.

Shaw, C. L., & Kennedy, D. A. (2021). What the Reproductive Number R0 can and cannot tell us about COVID-19 Dynamics. *Theoretical Population Biology*, *137*, 2–9.

Sierra-Rojas, J. C., Reyes-Carreto, R., Vargas-De-León, C., & Camacho, J. F. (2022). Modeling and Mathematical Analysis of the Dynamics of HPV in Cervical Epithelial Cells: Transient, Acute, Latency, and Chronic Infections. *Computational and Mathematical Methods in Medicine*, *2022*.

Smith, R. J., Li, J., & Blakeley, D. (2011). The failure of R0. *Computational and Mathematical Methods in Medicine*, *2011*.

Stark, H., & Zivković, A. (2018). HPV Vaccination: Prevention of Cervical Cancer in Serbia and in Europe. *Acta Facultatis Medicae Naissensis*, *35*(1), 5–16.

Tabassum, S., Rosli, N. B., & Binti Mazalan, M. S. A. (2019). Mathematical Modeling of Cancer Growth Process: A Review. *Journal of Physics: Conference Series*, *1366*(1).

Verma, M., Erwin, S., Abedi, V., Hontecillas, R., Hoops, S., Leber, A., Bassaganya-Riera, J., & Ciupe, S. M. (2017). Modeling the mechanisms by which HIV Associated immunosuppression influences HPV persistence at the Oral Mucosa. *PLoS ONE*, *12*(1), 1–20.

Weiss, H. (2009). A Mathematical Introduction to Population Dynamics. *Colóquio Brasileiro de Matemática*, *27*, 185.

Zhang, K., Ji, Y., Pan, Q., Wei, Y., Ye, Y., & Liu, H. (2020). Sensitivity analysis and optimal treatment control for a mathematical model of human papillomavirus infection. *AIMS Mathematics*, *5*(3), 2646–2670.

APPENDICES

Appendix 1

Section 1.

The characteristic polynomial of the above matrix is given as;

$$a_0\lambda^6 + a_1\lambda^5 + a_2\lambda^4 + a_3\lambda^3 + a_4\lambda^2 + a_5\lambda + a_6 = 0,$$

Where constant $a_0, a_{1,} a_{2,} a_{3,} a_{4,} a_5, a_6$ are determined using Mathematica software as;

Routh Table

Label				
λ^6	1	a_2	a_4	a_6
λ^5	a_1	a_3	a_5	0
λ^4	b_1	b_2	b_3	0
λ^3	c_1	c_2	0	0
λ^2	d_1	d_2	0	0
λ^1	e_1	0	0	0
λ^0	f_1	0	0	0

Appendix 1: Routh table

Where,

$$b_1 = \frac{-\begin{vmatrix} 1 & a_2 \\ a_1 & a_3 \end{vmatrix}}{a_1} = \frac{a_1a_2 - a_3}{a_1} \qquad b_2 = \frac{-\begin{vmatrix} 1 & a_4 \\ a_1 & a_5 \end{vmatrix}}{a_1} = \frac{a_1a_4 - a_5}{a_1} \qquad b_3 = \frac{-\begin{vmatrix} 1 & a_6 \\ a_1 & 0 \end{vmatrix}}{a_1} = a_6$$

$$c_1 = \frac{-\begin{vmatrix} a_1 & a_3 \\ b_1 & b_2 \end{vmatrix}}{b_1} = \frac{b_1a_3 - a_1b_2}{b_1} \qquad c_2 = \frac{-\begin{vmatrix} a_1 & a_5 \\ b_1 & b_3 \end{vmatrix}}{b_1} = \frac{b_1a_5 - a_1b_3}{b_1} \qquad d_1 = \frac{-\begin{vmatrix} b_1 & b_2 \\ c_1 & c_2 \end{vmatrix}}{c_1} = \frac{c_1b_2 - b_1c_2}{c_1}$$

$$d_2 = \frac{-\begin{vmatrix} b_1 & b_3 \\ c_1 & 0 \end{vmatrix}}{c_1} = b_3 \qquad e_1 = \frac{-\begin{vmatrix} c_1 & c_2 \\ d_1 & d_2 \end{vmatrix}}{d_1} = \frac{d_1 c_2 - c_1 d_2}{d_1} \qquad f_1 = -\begin{vmatrix} d_1 & d_2 \\ \frac{e_1}{d_1} & 0 \end{vmatrix} = \frac{d_2 e_1}{d_1}$$

Section 2.

$$\begin{aligned} a_1 = \frac{1}{S^0(L^0 + K_4)} (& S^0(\epsilon L^0 - L^0 r_2 - K_4 r_2 + L^0 \delta_2 + K_4 \delta_2 + (-L^0 - K_4)(r_1 - S^0 k_1 r_1 \\ & + (1 - S^0 k_1) r_1 - \Omega_2 - \Omega_3)) - S^0(L^0 + K_4)((1 - S^0 k_1) r_1 - \Omega_4) \\ & + S^0(L^0 + K_4)(\delta_1 + \delta_3 + k_3(1 - L^0 k_3) r_3 L^{0\prime} + k_1 r_1 S^{0\prime} - S^0 k_1^2 r_1 S^{0\prime})) \end{aligned}$$

$$\begin{aligned} a_2 = \frac{1}{S(L^0 + K_4)} (& -AB(-L^0 - K_4)\eta_1 \omega_1 + S^0((-L^0 - K_4)(-r_1 + S^0 k_1 r_1 + \Omega_2)((1 \\ & - S^0 k_1) r_1 - \Omega_3) + (-L^0 \epsilon + L^0 r_2 + K_4 r_2 - L^0 \delta_2 - K_4 \delta_2)(r_1 - S^0 k_1 r_1 \\ & + (1 - S^0 k_1) r_1 - \Omega_2 - \Omega_3)) - S^0(L^0 \epsilon - L^0 r_2 - K_4 r_2 + L^0 \delta_2 + K_4 \delta_2 \\ & + (-L^0 - K_4)(r_1 - S^0 k_1 r_1 + (1 - S^0 k_1) r_1 - \Omega_2 - \Omega_3))((1 - S^0 k_1) r_1 \\ & - \Omega_4) + (S^0(L^0 \epsilon - L^0 r_2 - K_4 r_2 + L^0 \delta_2 + K_4 \delta_2 + (-L^0 - K_4)(r_1 \\ & - S^0 k_1 r_1 + (1 - S^0 k_1) r_1 - \Omega_2 - \Omega_3)) - S^0(L^0 + K_4)((1 - S^0 k_1) r_1 \\ & - \Omega_4))(\delta_1 + \delta_3 + k_3(1 - L^0 k_3) r_3 L^{0\prime} + k_1 r_1 S^{0\prime} - S^0 k_1^2 r_1 S^{0\prime}) + S^0(L^0 \\ & + K_4)(-\delta_3 - k_3(1 - L^0 k_3) r_3 L^{0\prime})(-\delta_1 - k_1 r_1 S^{0\prime} + S^0 k_1^2 r_1 S^{0\prime})) \end{aligned}$$

$$a_3 = \frac{1}{S^0(L^0+K_4)}(\tau_2 B(\beta(L^0+K_4)\eta_2\omega_2 + (-L^0-K_4)\eta_1\omega_1((1-S^0k_1)r_1-\Omega_3))$$
$$+ S^0(-L^0\epsilon + L^0r_2 + K_4r_2 - L^0\delta_2 - K_4\delta_2)(-r_1 + S^0k_1r_1 + \Omega_2)((1$$
$$- S^0k_1)r_1 - \Omega_3) + (\tau_2 B(-L^0-K_4)\eta_1\omega_1 - S^0((-L^0-K_4)(-r_1$$
$$+ S^0k_1r_1 + \Omega_2)((1-S^0k_1)r_1-\Omega_3) + (-L^0\epsilon + L^0r_2 + K_4r_2 - L^0\delta_2$$
$$- K_4\delta_2)(r_1 - S^0k_1r_1 + (1-S^0k_1)r_1 - \Omega_2 - \Omega_3)))((1-S^0k_1)r_1-\Omega_4)$$
$$+ (-AB(-L^0-K_4)\eta_1\omega_1 + S^0((-L^0-K_4)(-r_1 + S^0k_1r_1 + \Omega_2)((1$$
$$- S^0k_1)r_1 - \Omega_3) + (-L^0\epsilon + L^0r_2 + K_4r_2 - L^0\delta_2 - K_4\delta_2)(r_1 - S^0k_1r_1$$
$$+ (1-S^0k_1)r_1 - \Omega_2 - \Omega_3)) - S^0(L^0\epsilon - L^0r_2 - K_4r_2 + L^0\delta_2 + K_4\delta_2$$
$$+ (-L^0-K_4)(r_1 - S^0k_1r_1 + (1-S^0k_1)r_1 - \Omega_2 - \Omega_3))((1-S^0k_1)r_1$$
$$- \Omega_4))(\delta_1 + \delta_3 + k_3(1-L^0k_3)r_3L^{0\prime} + k_1r_1S^{0\prime} - S^0k_1^2r_1S^{0\prime})$$
$$+ (S^0(L^0\epsilon - L^0r_2 - K_4r_2 + L^0\delta_2 + K_4\delta_2 + (-L^0-K_4)(r_1 - S^0k_1r_1$$
$$+ (1-S^0k_1)r_1 - \Omega_2 - \Omega_3)) - S^0(L^0+K_4)((1-S^0k_1)r_1-\Omega_4))(-\delta_3$$
$$- k_3(1-L^0k_3)r_3L^{0\prime})(-\delta_1 - k_1r_1S^{0\prime} + S^0k_1^2r_1S^{0\prime}))$$

$$a_4 = \frac{1}{S^0(L^0+K_4)}((-AB(\beta(L^0+K_4)\eta_2\omega_2 + (-L^0-K_4)\eta_1\omega_1((1-S^0k_1)r_1-\Omega_3))$$
$$- S^0(-L^0\epsilon + L^0r_2 + K_4r_2 - L^0\delta_2 - K_4\delta_2)(-r_1 + S^0k_1r_1 + \Omega_2)((1$$
$$- S^0k_1)r_1 - \Omega_3))((1-S^0k_1)r_1-\Omega_4) + (AB(\beta(L^0+K_4)\eta_2\omega_2 + (-L^0$$
$$- K_4)\eta_1\omega_1((1-S^0k_1)r_1-\Omega_3)) + S^0(-L^0\epsilon + L^0r_2 + K_4r_2 - L^0\delta_2$$
$$- K_4\delta_2)(-r_1 + S^0k_1r_1 + \Omega_2)((1-S^0k_1)r_1-\Omega_3) + (AB(-L^0$$
$$- K_4)\eta_1\omega_1 - S^0((-L^0-K_4)(-r_1 + S^0k_1r_1 + \Omega_2)((1-S^0k_1)r_1-\Omega_3)$$
$$+ (-L^0\epsilon + L^0r_2 + K_4r_2 - L^0\delta_2 - K_4\delta_2)(r_1 - S^0k_1r_1 + (1-S^0k_1)r_1$$
$$- \Omega_2 - \Omega_3)))((1-S^0k_1)r_1-\Omega_4))(\delta_1 + \delta_3 + k_3(1-L^0k_3)r_3L^{0\prime}$$
$$+ k_1r_1S^{0\prime} - S^0k_1^2r_1S^0) + (-AB(-L^0-K_4)\eta_1\omega_1 + S^0((-L^0-K_4)(-r_1$$
$$+ S^0k_1r_1 + \Omega_2)((1-S^0k_1)r_1-\Omega_3) + (-L^0\epsilon + L^0r_2 + K_4r_2 - L^0\delta_2$$
$$- K_4\delta_2)(r_1 - S^0k_1r_1 + (1-S^0k_1)r_1 - \Omega_2 - \Omega_3)) - S^0(L^0\epsilon - L^0r_2$$
$$- K_4r_2 + L^0\delta_2 + K_4\delta_2 + (-L^0-K_4)(r_1 - S^0k_1r_1 + (1-S^0k_1)r_1 - \Omega_2$$
$$- \Omega_3))((1-S^0k_1)r_1-\Omega_4))(-\delta_3 - k_3(1-L^0k_3)r_3L^{0\prime})(-\delta_1 - k_1r_1S^{0\prime}$$
$$+ S^0k_1^2r_1S^{0\prime}))$$

$$a_5 = \frac{1}{S^0(L^0+K_4)}((-\tau_2 AB(\beta(L^0+K_4)\eta_2\omega_2 + (-L^0-K_4)\eta_1\omega_1((1-S^0k_1)r_1 - \Omega_3)) - S^0(-L^0\epsilon + L^0r_2 + K_4r_2 - L^0\delta_2 - K_4\delta_2)(-r_1 + S^0k_1r_1 + \Omega_2)((1-S^0k_1)r_1 - \Omega_3))((1-S^0k_1)r_1 - \Omega_4)(\delta_1 + \delta_3 + k_3(1-L^0k_3)r_3L^{0\prime} + k_1r_1S^{0\prime} - S^0k_1^2r_1S^{0\prime}) + (\tau_2 B(\beta(L^0+K_4)\eta_2\omega_2 + (-L^0-K_4)\eta_1\omega_1((1-S^0k_1)r_1 - \Omega_3)) + S^0(-L^0\epsilon + L^0r_2 + K_4r_2 - L^0\delta_2 - K_4\delta_2)(-r_1 + S^0k_1r_1 + \Omega_2)((1-S^0k_1)r_1 - \Omega_3) + (\tau_2 B(-L^0 - K_4)\eta_1\omega_1 - S^0((-L^0-K_4)(-r_1 + S^0k_1r_1 + \Omega_2)((1-S^0k_1)r_1 - \Omega_3) + (-L^0\epsilon + L^0r_2 + K_4r_2 - L^0\delta_2 - K_4\delta_2)(r_1 - S^0k_1r_1 + (1-S^0k_1)r_1 - \Omega_2 - \Omega_3)))((1 - S^0k_1)r_1 - \Omega_4))(-\delta_3 - k_3(1-L^0k_3)r_3LL^{0\prime})(-\delta_1 - k_1r_1S^0S^{0\prime} + S^0k_1^2r_1S^{0\prime}))$$

$$a_6 = \frac{1}{S^0(L^0+K_4)}(-\tau_2 B(\beta(L^0+K_4)\eta_2\omega_2 + (-L^0-K_4)\eta_1\omega_1((1-S^0k_1)r_1 - \Omega_3)) - S^0(-L^0\epsilon + L^0r_2 + K_4r_2 - L^0\delta_2 - K_4\delta_2)(-r_1 + S^0k_1r_1 + \Omega_2)((1 - S^0k_1)r_1 - \Omega_3))((1-S^0k_1)r_1 - \Omega_4)(-\delta_3 - k_3(1-L^0k_3)r_3L^{0\prime})(-\delta_1 - k_1r_1S^{0\prime} + S^0k_1^2r_1S^{0\prime})$$

By Routh-Hurwitz criteria for stability, the system (1) – (6) is locally asymptomatically stable at disease-free equilibrium (E^0) if and only if $a_1 > 0, a_2 > 0, a_4 > 0, a_6 > 0, b_1 > 0, c_1 > 0, d_1 > 0\ and\ e_1 > 0$ are satisfied and otherwise unstable.

Section 3.

The bifurcation results of a and b values are as follows;

$$
\begin{aligned}
a = -(&2(-AB + u\_2)v\_3\,\eta\_2\,\omega\_2\,(-(\epsilon f\_6)/(f\_6 + K\_4\,) + (1 - f\_5/K\_2\,)r\_2 - \delta\_2 + (1 \\
&- f\_5/K\_2\,)\eta\_1\,\omega\_1 - (f\_5\,r\_2 + f\_2\,\eta\_1\,\omega\_1 + f\_3\,\eta\_2\,\omega\_2 \\
&+ f\_4\,\eta\_3\,\omega\_3)/K\_2\,)(\beta u\_3 - u\_5\,[\eta\_1\,\omega\_1]))/((\epsilon/(1 + k\_4\,) + r\_2 \\
&- \delta\_2)(\varepsilon/(1 + K\_4\,) + r\_2 - \delta\_2)(-1 + \beta + k\_1 - \delta\_1 - \eta\_1 + \Omega\_1)) \\
&+ (2(-AB + u\_2)v\_3\,\eta\_2\,\omega\_2\,(-(\epsilon f\_6)/(f\_6 + K\_4\,) + (1 - f\_5/K\_2\,)r\_2 \\
&- \delta\_2 + (1 - f\_5/K\_2\,)\eta\_2\,\omega\_2 - (f\_5\,r\_2 + f\_2\,\eta\_1\,\omega\_1 + f\_3\,\eta\_2\,\omega\_2 \\
&+ f\_4\,\eta\_3\,\omega\_3)/K\_2\,)u\_5\,[\eta\_3\,\omega\_3])/((\epsilon/(1 + k\_4\,) + r\_2 - \delta\_2)(\varepsilon/(1 \\
&+ K\_4\,) + r\_2 - \delta\_2)((1 - k\_1)r\_1 - \eta\_3)) + (2(-AB \\
&+ u\_2)v\_3\,\eta\_2\,\omega\_2\,(-(\epsilon f\_6)/(f\_6 + K\_4\,) + (1 - f\_5/K\_2\,)r\_2 - \delta\_2 + (1 \\
&- f\_5/K\_2\,)\eta\_3\,\omega\_3 - (f\_5\,r\_2 + f\_2\,\eta\_1\,\omega\_1 + f\_3\,\eta\_2\,\omega\_2 \\
&+ f\_4\,\eta\_3\,\omega\_3)/K\_2\,)u\_5\,[\eta\_3\,\omega\_3])/((\epsilon/(1 + k\_4\,) + r\_2 - \delta\_2)(\varepsilon/(1 \\
&+ K\_4\,) + r\_2 - \delta\_2)((1 - k\_1)r\_1 - \eta\_4)) - (2ABv\_5\,(\beta \\
&+ (2\theta f\_3\text{\^{}3}\,f\_4)/〚(D\text{\^{}2} + f\_3\text{\^{}2})〛\text{\^{}2} - (2\theta f\_3\,f\_4)/(D\text{\^{}2} + f\_3\text{\^{}2}\,) \\
&+ 1[1 - N/K\_1\,]r\_1 - \delta\_1 - \eta\_2)(\beta u\_3 \\
&- u\_5\,[\eta\_1\,\omega\_1])u\_5\,[\eta\_3\,\omega\_3])/(〚((1 - k\_1)r\_1 - \eta\_3)〛\text{\^{}2}\,(-1 + \beta \\
&+ k\_1 - \delta\_1 - \eta\_1 + \Omega\_1)) - (2AB(\beta - (\theta f\_3\text{\^{}2})/(D\text{\^{}2} \\
&+ f\_3\text{\^{}2}\,))v\_5\,(\beta u\_3 - u\_5\,[\eta\_1\,\omega\_1])u\_5\,[\eta\_3\,\omega\_3])/(((1 - k\_1)r\_1 \\
&- \eta\_3)((1 - k\_1)r\_1 - \eta\_4)(-1 + \beta + k\_1 - \delta\_1 - \eta\_1 + \Omega\_1)) \\
&+ (2v\_3\,\eta\_2\,\omega\_2\,((1 - f\_5/K\_2\,)\eta\_1\,\omega\_1 + (1 - f\_5/K\_2\,)\eta\_2\,\omega\_2)(\beta u\_3 \\
&- u\_5\,[\eta\_1\,\omega\_1])u\_5\,[\eta\_3\,\omega\_3])/((\varepsilon/(1 + K\_4\,) + r\_2 - \delta\_2)((1 - k\_1)r\_1 \\
&- \eta\_3)(-1 + \beta + k\_1 - \delta\_1 - \eta\_1 + \Omega\_1)) + (2v\_3\,\eta\_2\,\omega\_2\,((1 \\
&- f\_5/K\_2\,)\eta\_1\,\omega\_1 + (1 - f\_5/K\_2\,)\eta\_3\,\omega\_3)(\beta u\_3 \\
&- u\_5\,[\eta\_1\,\omega\_1])u\_5\,[\eta\_3\,\omega\_3])/((\varepsilon/(1 + K\_4\,) + r\_2 - \delta\_2)((1 - k\_1)r\_1 \\
&- \eta\_4)(-1 + \beta + k\_1 - \delta\_1 - \eta\_1 + \Omega\_1)) + (2ABv\_5\,(-(\theta f\_3\text{\^{}2})/(D\text{\^{}2} \\
&+ f\_3\text{\^{}2}\,) + (2\theta f\_3\text{\^{}3}\,f\_4)/〚(D\text{\^{}2} + f\_3\text{\^{}2})〛\text{\^{}2} - (2\theta f\_3\,f\_4)/(D\text{\^{}2} \\
&+ f\_3\text{\^{}2}\,) + 1[1 - N/K\_1\,]r\_1 - \delta\_1 - \eta\_2)\,〚u\_5\,[\eta\_3\,\omega\_3]〛\text{\^{}2})/(〚((1 \\
&- k\_1)r\_1 - \eta\_3)〛\text{\^{}2}\,((1 - k\_1)r\_1 - \eta\_4)) - (2v\_3\,\eta\_2\,\omega\_2\,((1 \\
&- f\_5/K\_2\,)\eta\_2\,\omega\_2 + (1 \\
&- f\_5/K\_2\,)\eta\_3\,\omega\_3)\,〚u\_5\,[\eta\_3\,\omega\_3]〛\text{\^{}2})/((\varepsilon/(1 + K\_4\,) + r\_2 - \delta\_2)((1 \\
&- k\_1)r\_1 - \eta\_3)((1 - k\_1)r\_1 - \eta\_4)) - (2(-\tau\_2\,B + u\_2)(-k\_1\,r\_1\,v\_4 \\
&+ \tau\_2\,Bv\_5 + v\_2\,(k\_1\,r\_1 - \eta\_1))u\_5\,[\eta\_1\,\omega\_1](eM/(F + M) \\
&+ (\tau\_2\,Bf\_1)/〚(f\_1 + Bf\_5)〛\text{\^{}2} - (r\_1\ 〚f\_1〛\text{\^{}}'\,[1 - (f\_1 + f\_2 + f\_3 \\
&+ f\_4)/K\_1\,])/K\_1\,))/(((1 - k\_1)r\_1 - k\_1\,r\_1 - \delta\_1)(\epsilon/(1 + k\_4\,) + r\_2
\end{aligned}
$$

$$-\delta\_2-\tau\_2)(-1+\beta+k\_1-\delta\_1-\eta\_1+\Omega\_1))\}$$

$$b$$

$$=\frac{2\theta f_3^3 f_4}{(D^2+f_3^2)^2}-\frac{2\theta f_3 f_4}{D^2+f_3^2}-\delta_1-\eta_2$$

$$+\frac{(-AB+u_2)(k_1r_1v_3+ABv_5)(\frac{ABf_1}{(f_1+Bf_5)^2}+f_1[1-\frac{f_1+f_2+f_3+f_4}{K_1}])}{((1-k_1)r_1-k_1r_1-\delta_1)(\frac{\epsilon}{1+k_4}+r_2-\delta_2)}+f_3[1$$

$$-\frac{f_1+f_2+f_3+f_4}{K_1}]+\frac{AB(-AB+u_2)v_5f_3[1-\frac{f_1+f_2+f_3+f_4}{K_1}]}{(\frac{\epsilon}{1+k_4}+r_2-\delta_2)((1-k_1)r_1-\eta_3)}$$

$$+\frac{AB(\beta+f_3(1-\frac{f_1+f_2+f_3+f_4}{K_1})-\frac{f_3r_1}{K_1})v_5(\beta u_3-u_5[\eta_1\omega_1])}{((1-k_1)r_1-\eta_3)(-1+\beta+k_1-\delta_1-\eta_1+\Omega_1)}$$

$$-\frac{(k_1r_1v_3+ABv_5)u_5[\eta_3\omega_3](f_1[1-\frac{f_1+f_2+f_3+f_4}{K_1}]-\frac{r_1f_1'[1-\frac{f_1+f_2+f_3+f_4}{K_1}]}{K_1})}{((1-k_1)r_1-k_1r_1-\delta_1)((1-k_1)r_1-\eta_3)}$$

$$-\frac{(k_1r_1v_3+ABv_5)u_5[\eta_3\omega_3](f_1[1-\frac{f_1+f_2+f_3+f_4}{K_1}]-\frac{r_1f_1'[1-\frac{f_1+f_2+f_3+f_4}{K_1}]}{K_1})}{((1-k_1)r_1-k_1r_1-\delta_1)((1-k_1)r_1-\eta_4)}$$

$$+\frac{(k_1r_1v_3+ABv_5)(\beta u_3-u_5[\eta_1\omega_1])(\frac{eM}{F+M}+f_1[1-\frac{f_1+f_2+f_3+f_4}{K_1}]-\frac{r_1f_1'[1-\frac{f_1+f_2+f_3+f_4}{K_1}]}{K_1})}{((1-k_1)r_1-k_1r_1-\delta_1)(-1+\beta+k_1-\delta_1-\eta_1+\Omega_1)}$$

$$-\frac{ABr_1v_5u_5[\eta_3\omega_3](1[1-\frac{f_1+f_2+f_3+f_4}{K_1}]-\frac{f_3'[1-\frac{f_1+f_2+f_3+f_4}{K_1}]}{K_1})}{((1-k_1)r_1-\eta_3)^2}$$

$$-\frac{ABv_5u_5[\eta_3\omega_3](-\frac{\theta f_3^2}{D^2+f_3^2}+f_3[1-\frac{f_1+f_2+f_3+f_4}{K_1}]-\frac{r_1f_3'[1-\frac{f_1+f_2+f_3+f_4}{K_1}]}{K_1})}{((1-k_1)r_1-\eta_3)((1-k_1)r_1-\eta_4)}$$

Section 4.

$$b_4 = 1;$$

$$b_3 = r_1\left(-\frac{1}{\frac{MQ}{F+M}+\beta+\delta_1+\eta_1}-\frac{1}{\delta_1+\eta_2}-\frac{1}{\delta_1+\eta_3}\right.$$
$$\left.+\frac{S\left(\frac{1}{\frac{MQ}{F+M}+\beta+\delta_1+\eta_1}+\frac{1}{\delta_1+\eta_2}+\frac{1}{\delta_1+\eta_3}\right)}{K_1}\right)-\frac{r_2}{\frac{L\epsilon}{L+K_4}+\delta_2+S\tau_1}$$

$$b\_2 = r\_1\ ((\llbracket(S-K\_1)\rrbracket\hat{}2\ r\_1\ (F\beta+M(Q+\beta)+(F+M)(3\delta\_1+\eta\_1+\eta\_2$$
$$+\eta\_3)))/(K\_1\hat{}2\ (F\beta+M(Q+\beta)+(F+M)(\delta\_1+\eta\_1))(\delta\_1$$
$$+\eta\_2)(\delta\_1+\eta\_3))+(r\_2\ (1/(MQ/(F+M)+\beta+\delta\_1+\eta\_1\ )$$
$$+1/(\delta\_1+\eta\_2\ )+1/(\delta\_1+\eta\_3\ )+(S(-1/(MQ/(F+M)+\beta+\delta\_1$$
$$+\eta\_1\ )-1/(\delta\_1+\eta\_2\ )-1/(\delta\_1+\eta\_3\ )))/K\_1\ ))/(L\epsilon/(L+K\_4\ )$$
$$+\delta\_2+S\tau\_1\ ))$$

$$b_1 = -\frac{r_1^3}{\left(\frac{MQ}{F+M}+\beta+\delta_1+\eta_1\right)(\delta_1+\eta_2)(\delta_1+\eta_3)}+\frac{S^3r_1^3}{K_1^3\left(\frac{MQ}{F+M}+\beta+\delta_1+\eta_1\right)(\delta_1+\eta_2)(\delta_1+\eta_3)}-$$
$$\frac{3S^2r_1^3}{K_1^2\left(\frac{MQ}{F+M}+\beta+\delta_1+\eta_1\right)(\delta_1+\eta_2)(\delta_1+\eta_3)}+\frac{3Sr_1^3}{K_1\left(\frac{MQ}{F+M}+\beta+\delta_1+\eta_1\right)(\delta_1+\eta_2)(\delta_1+\eta_3)}-$$
$$\frac{r_1^2r_2}{\left(\frac{MQ}{F+M}+\beta+\delta_1+\eta_1\right)(\delta_1+\eta_2)\left(\frac{L\epsilon}{L+K_4}+\delta_2+S\tau_1\right)}-\frac{S^2r_1^2r_2}{K_1^2\left(\frac{MQ}{F+M}+\beta+\delta_1+\eta_1\right)(\delta_1+\eta_2)\left(\frac{L\epsilon}{L+K_4}+\delta_2+S\tau_1\right)}+$$
$$\frac{2Sr_1^2r_2}{K_1\left(\frac{MQ}{F+M}+\beta+\delta_1+\eta_1\right)(\delta_1+\eta_2)\left(\frac{L\epsilon}{L+K_4}+\delta_2+S\tau_1\right)}-\frac{r_1^2r_2}{\left(\frac{MQ}{F+M}+\beta+\delta_1+\eta_1\right)(\delta_1+\eta_3)\left(\frac{L\epsilon}{L+K_4}+\delta_2+S\tau_1\right)}-$$
$$\frac{S^2r_1^2r_2}{K_1^2\left(\frac{MQ}{F+M}+\beta+\delta_1+\eta_1\right)(\delta_1+\eta_3)\left(\frac{L\epsilon}{L+K_4}+\delta_2+S\tau_1\right)}+\frac{2Sr_1^2r_2}{K_1\left(\frac{MQ}{F+M}+\beta+\delta_1+\eta_1\right)(\delta_1+\eta_3)\left(\frac{L\epsilon}{L+K_4}+\delta_2+S\tau_1\right)}-$$
$$\frac{r_1^2r_2}{(\delta_1+\eta_2)(\delta_1+\eta_3)\left(\frac{L\epsilon}{L+K_4}+\delta_2+S\tau_1\right)}-\frac{S^2r_1^2r_2}{K_1^2(\delta_1+\eta_2)(\delta_1+\eta_3)\left(\frac{L\epsilon}{L+K_4}+\delta_2+S\tau_1\right)}+$$
$$\frac{2Sr_1^2r_2}{K_1(\delta_1+\eta_2)(\delta_1+\eta_3)\left(\frac{L\epsilon}{L+K_4}+\delta_2+S\tau_1\right)}.$$

$$b_0 = \frac{(F+M)(S^0-K_1)^3(L^0+K_4)r_1^3r_2}{K_1^3(F\beta+M(Q+\beta)+(F+M)(\delta_1+\eta_1))(\delta_1+\eta_2)(\delta_1+\eta_3)(L^0\epsilon+(L^0+K_4)(\delta_2+S\tau_1))}$$